Armel Koulong[1]
Department of Mechanical Engineering,
University of Alabama,
245 7th Ave,
Tuscaloosa, Alabama, USA
email: akoulongzoyem@crimson.ua.edu

Ali Pakniyat
Multi-Modal Multi-Agent Control ($\mathcal{M}^3\mathcal{AC}$)
Lab, Department of Mechanical Engineering,
University of Alabama,
Tuscaloosa, AL 35401 USA
email: apakniyat@ua.edu

Distributed Leader-Follower Consensus for Uncertain Multi-agent Systems with Time-Triggered Switching of the Communication Network

A distributed adaptive control strategy is developed for heterogeneous multi-agent systems in nonlinear Brunovsky form with p-dimensional n^{th}-order dynamics, operating under time-triggered switching communication topologies. The approach integrates bounded proximity-dependent repulsive potential functions for agent-agent, agent-leader, and agent-obstacle proximity management with neural-network estimators for compensating system uncertainties and disturbances. The resulting distributed control and adaptive laws, together with dwell-time requirements for topology transitions, achieve leader-following consensus. This integrated design provides synchronized formation and robust disturbance rejection in evolving network configurations, and its effectiveness is demonstrated through multiple numerical simulations.

Keywords: Multi-agent and Networked System, Adaptive and Learning Systems, Nonlinear Control Systems

Nomenclature

- a_{ij}^{σ} = Adjacency weight from agent j to i in mode σ.
- A^{σ} = Weighted adjacency matrix of $\mathcal{G}^{\sigma}$.
- D^{σ} = In-degree matrix $\mathrm{diag}\big(\sum_j a_{ij}^{\sigma}\big)$.
- L^{σ} = Graph Laplacian of $\mathcal{G}^{\sigma}$.
- $\mathbb{R}$ = Set of real numbers.
- $\mathbb{R}^p$ = Set of real vectors of dimension p.
- λ_{ij} = Synchronization-error weight between agents i and j.
- ψ_{ij}^1 = Minimum separation (collision-avoidance threshold) between agents i and j.
- ψ_{i0}^1 = Minimum separation (collision-avoidance threshold) between agent i and the leader.
- R = Outer safety radius around an obstacle (threshold distance).
- $\mathfrak{L}$ = Inner exclusion radius around an obstacle (threshold distance).
- ϖ = Inter-agent/leader repulsion strength.
- κ_i = Scalar tuning gain in NN update laws.
- κ_0 = Scalar tuning gain in NN update laws.
- κ_{iw} = Scalar tuning gain in NN update laws.
- Γ^0 = Gain matrix scaling obstacle/collision-avoidance inputs.
- Γ^1 = Gain matrix scaling obstacle/collision-avoidance inputs.
- Γ^2 = Gain matrix scaling obstacle/collision-avoidance inputs.
- $\mathrm{tr}\{\cdot\}$ = Trace of a matrix.
- $t \in \mathbb{R}_{\geq 0}$ = Continuous time.
- $|\cdot|$ = Absolute value.
- $\|\cdot\|$ = Euclidean (vector 2-)norm.
- $\|\cdot\|_G$ = Frobenius norm for matrices.
- P^{-1} = Inverse of matrix $P^{\sigma(t)}$.
- t_s = Switching instant.
- t_s^- = Time immediately before the switching instant.
- $\alpha(\cdot)$ = Singular values.
- $\bar{\alpha}(\cdot)$ = Maximal singular values.
- $\underline{\alpha}(\cdot)$ = Minimal singular values.
- m_{ij} = Repulsive potential for agent–agent interaction.
- m_{i0} = Repulsive potential for agent–leader interaction.
- $m_{i\mathfrak{c}}$ = Repulsive potential for agent–obstacle interaction.
- $\mathcal{G}^{\sigma} = (\mathcal{V}, \mathcal{E}^{\sigma})$ = Communication graph under mode σ.
- $\bar{\mathcal{G}}^{\sigma}$ = Augmented graph including leader node 0.
- $\hat{\theta}_i$ = Estimated neural weights for agent i.
- $\hat{\theta}_{iw}$ = Estimated neural weights for the disturbance on agent i.
- $\hat{\theta}_0$ = Estimated neural weights for the leader.
- δ_{ij} = Positive lower bound on the initial separation between agents i and j.
- δ_{i0} = Positive lower bound on the initial separation between agent i and the leader.
- X_{init} = Upper bound on the norm of any agent's initial state.
- $f_{\mathrm{init}}(\cdot)$ = Continuous function bounding each $f_i(x)$ on a compact set.
- $f_0(x_0)$ = Continuous function bounding the leader's dynamics $f_0(x_0)$.
- w_{init} = Upper bound on the norm of the disturbance.
- $\mathbb{R}^{(N\cdot p)\times(N\cdot p)}$ = Set of real matrices with $(N\cdot p)$ rows and $(N\cdot p)$ columns.
- $G_i \in \mathbb{R}^{q_i\times q_i}$ = Positive definite adaptation-gain matrix for the NN of agent-dynamics.
- $G_{i0} \in \mathbb{R}^{q_0\times q_0}$ = Positive definite adaptation-gain matrix for the NN of leader-dynamics.
- $G_{iw} \in \mathbb{R}^{q_{iw}\times q_{iw}}$ = Positive definite adaptation-gain matrix for the NN of disturbance model.

[1]Corresponding Author.
Version 1.18, May 30, 2026

1 Introduction

The cooperative control of multi-agent systems (MAS) is essential for applications such as unmanned aerial vehicle (UAV) coordination, autonomous vehicle platooning, and smart grids. In these systems, agents interact only with a limited number of other agents, creating a graph-theoretic structure that complicates achieving global consensus [1,2]. This challenge is further amplified in heterogeneous uncertain MAS, where agents with different forms of high-order non-linear dynamics are subject to external disturbances [3]. Moreover, adapting to unknown parameters in real-time further complicates the consensus process, as agents must continuously update their internal models based on limited interactions.

Despite advancements in the field, significant gaps remain in addressing adaptive control for leader-following consensus with obstacle and collision avoidance in nonlinear systems. Foundational works have addressed these challenges in isolation, but no single framework provides an integrated solution. For instance, adaptive tracking control methods [1,4] and consensus approaches for switching communication topologies [5] often neglect physical constraints like collision avoidance. Furthermore, while the adaptive tracking method in [4] effectively handles switching topologies, its formulation is limited to linear agent dynamics and does not extend to heterogeneous nonlinear MAS. Conversely, research that does consider safety—such as work on local interaction rules [6], optimal control for consensus [7], and geometric formation conditions [8]—often overlooks the complexities of nonlinear dynamics, adaptation, and network switching. Stability analyses for time-dependent links [9] and switching topologies [10] highlight network challenges but only partially address physical constraints and heterogeneous dynamics, while ignoring the need for real-time nonlinear estimation.

Recent research in the past few years has significantly sharpened the landscape for adaptive multi-agent systems under switching communication topologies. Some studies explore consensus for unknown nonlinear MAS with communication noise under Markov switching, using Radial Basis Function networks and stochastic stability conditions [11]; these efforts focus on state consensus without addressing formation, safety, or average dwell time (ADT) considerations. Other work investigates positive consensus for linear MAS with ADT switching, establishing infimum dwell times and positivity-preserving conditions for consensus but without encompassing nonlinearity, heterogeneity, adaptations to uncertainty, or safety aspects [12].

Event-triggered designs have also been proposed; some researchers have introduced decentralized protocols with dynamic event triggering and guaranteed minimum inter-event times to improve robustness and communication efficiency [13], and others have developed neural adaptive event-triggered consensus methods for unknown nonlinear MAS on switched or Markovian networks [14]. However, these references do not study safety guarantees or explicit dwell time constraints, as their approaches prioritize consensus and communication.

In the context of formation control under switching topologies, research has often been tailored to address the requirements of specific applications. For instance, distributed adaptive robust schemes have been developed and experimentally validated for quadrotor UAVs, demonstrating effectiveness in outdoor environments [15]. Similarly, other studies have targeted formation control for fractional-order multi-agent systems with actuator faults [16], again focusing on the specific characteristics pertinent to those systems. Despite these advances in application-oriented domains, a comprehensive and unified framework that integrates heterogeneous higher-order agents, obstacle and collision avoidance via potential functions, distributed neural adaptation, and provable minimum average dwell time guarantees for leader-follower formation tracking remains unaddressed in the literature.

In the past work of the authors [17], we introduced an adaptive control strategy for multi-agent systems with fixed communication topology, focusing specifically on agents operating in a one-dimensional physical space. Due to the formulation adopted therein, the approach was limited to modeling collision avoidance scenarios restricted to one-dimensional interactions. In this paper, we extend the framework presented in [1,17] for heterogeneous multi-agent systems in the general Brunovsky form with p-dimensional nonlinear n^{th}-order dynamics operating under time-triggered switching communication topologies. A key distinguishing feature of this paper is the presentation of stability and convergence proofs that clearly establish conditions for cooperative uniform ultimate boundedness (CUUB), synchronization, and performance under topology switching.

The proposed methodology incorporates repulsion-based collision and obstacle mitigation under time-triggered switching communication topologies. Specifically, we integrate a distributed adaptive control architecture with a leader-follower formation structure, enabling heterogeneous multi-agent systems to achieve consensus and coordination despite evolving network configurations. To handle uncertainties arising from unknown agent dynamics and external disturbances, we employ neural network-based estimation techniques coupled with real-time adaptive tuning laws which continuously update the control parameters to ensure reliable performance under significant model uncertainties. Additionally, potential functions are incorporated to prevent close approaches while maintaining cohesive formations. In particular, we determine minimum average dwell-time conditions under which the closed-loop system achieves leader-follower synchronization and stability under switching communication topologies.

Building upon foundational work in single-agent switched systems [18,19], adaptive tracking [1], and various multi-agent consensus formulations for agents with linear dynamics—including consensus with obstacle and collision avoidance using local information under fixed topologies [7], as well as leader–follower consensus under variable topologies [4]—this paper presents a unified control framework for heterogeneous multi-agent systems with high-order Brunovsky nonlinear dynamics subject to switching communication topologies. To the best of our knowledge, no prior work provides a unified, decentralized design for such nonlinear systems that combines distributed linear-in-parameters (LIP)–neural network (NN) adaptation, time-triggered switching communication topologies, and potential-based repulsion mechanisms, together with a composite Lyapunov proof yielding explicit minimum average-dwell-time bounds for leader–follower formation tracking in heterogeneous p-dimensional, n-th-order Brunovsky systems.

The main contributions of this paper are:

(1) A unified, decentralized control architecture for heterogeneous, nonlinear multi-agent systems (MAS) that simultaneously addresses neural adaptation to uncertain dynamics, repulsion-based proximity management for collision/obstacle mitigation, and leader–follower formation consensus under switching communication topologies.
(2) A composite Lyapunov-based analysis that establishes explicit, topology- and parameter-dependent minimum average-dwell-time conditions for leader-follower formation tracking under switching communication topologies.
(3) Mathematical proofs of closed-loop stability, and cooperatively uniformly ultimately bounded tracking performance, with error bounds explicitly linked to tunable design parameters.
(4) A critical synthesis of foundational literature that overcomes the limitations of prior work—which addressed challenges like topology switching, safety and agent nonlinearity only in isolation—to deliver a unified decentralized framework for heterogeneous Brunovsky systems under switching communication topologies.

The remainder of the paper is structured as follows: Section 2 defines MAS dynamics, switching communication topology and the leader-following framework. Section 3 presents an adaptive control protocol with neural network-based learning for managing high dimensional non-linear dynamics and disturbances in a time-triggered switching network. Section 4 proves control law stability and convergence. Section 5 demonstrates the strategy via a numerical leader-follower example with switching communication topology. Section 6 summarizes contributions and potential future work.

2 Problem Formulation

We denote by $\mathcal{N} = \{1, 2, \ldots, N\}$ the set of N follower agents. Each follower's full state is $x_i = [x_i^1, x_i^2, \cdots, x_i^n]^\top \in \mathbb{R}^{n \cdot p}$, with $x_i^k \in \mathbb{R}^p$, $k = 1, 2, \ldots, n$, where p is the dimension of the physical space and x_i^k corresponds to the $(k-1)^{\text{th}}$ derivative of the agent's position (e.g., for two dimensional motions, $p = 2$, thus $x_i^k = \left[x_i^{k,1}, x_i^{k,2}\right]^\top \in \mathbb{R}^2$). The leader's state $x_0 \in \mathbb{R}^{n \cdot p}$ is partitioned similarly.

The dynamics of the i^{th} follower agent is described using the non-linear Brunovsky form as:

$$\begin{aligned} \dot{x}_i^1 &= x_i^2 \\ \dot{x}_i^2 &= x_i^3 \\ &\vdots \\ \dot{x}_i^n &= f_i(x_i) + u_i + w_i(t) \end{aligned} \tag{1}$$

where $u_i \in \mathbb{R}^p$ is the control input of agent i, and $w_i(t) \in \mathbb{R}^p$ denotes a bounded unknown time-varying disturbance affecting agent i.

We assume that the agent-specific functions $f_i(x_i) : \mathbb{R}^{n \cdot p} \to \mathbb{R}^p$ are unknown to the agents, but these functions are considered to be locally Lipschitz in x_i. For convenience in the Lyapunov stability analysis, we further adopt $f_i(0) = 0$ for all $i \in \mathcal{N}$; this assumption can be relaxed with appropriate changes in the analytical arguments (e.g., via invariance principles).

While the governing dynamics of Eqn. (1) of the agents are decoupled, their interactions become coupled through collision and obstacle avoidance, as discussed later in this section.

In discussions regarding the collective behavior of following agents, we utilize the Kronecker product [7] to collectively represent the dynamics of Eqn. (1) of all agents in the global form:

$$\begin{aligned} \dot{x}^1 &= x^2 \\ &\vdots \\ \dot{x}^n &= f(x) + u + w \end{aligned} \tag{2}$$

where $x^k = [x_1^k; x_2^k; \ldots; x_N^k] \in \mathbb{R}^{N \cdot p}$ denotes the concatenated k-th state vectors of all follower agents, $u = [u_1; u_2; \ldots; u_N] \in \mathbb{R}^{N \cdot p}$ denotes their control inputs, $w = [w_1; w_2; \ldots; w_N] \in \mathbb{R}^{N \cdot p}$ denotes unknown bounded disturbances, the unknown function $f(x) = [f_1(x_1); f_2(x_2); \ldots; f_N(x_N)] \in \mathbb{R}^{N \cdot p}$ collectively represents the non-linear dynamics of all N follower agents.

In the leader-follower scenario considered in this paper, the leader agent, denoted by subscript 0, generates a reference trajectory for follower agents, but this reference trajectory is a priori unknown to all follower agents, and the only information about the reference trajectory available to follower agents is the leader's state vector $x_0 \equiv x_0(t) \in \mathbb{R}^{n \cdot p}$ at the current time $t \in [t_0, \infty)$. The leader also determines a time-triggered switching rule for the communication topology as discussed later.

The time-varying dynamics of the leader agent is:

$$\begin{aligned} \dot{x}_0^1(t) &= x_0^2(t) \\ &\vdots \\ \dot{x}_0^n(t) &= f_0(x_0, t) \end{aligned} \tag{3}$$

where $x_0^k \in \mathbb{R}^p$ is the k-th partition of the leader agent's state, and $x_0 = [x_0^1, x_0^2, \ldots, x_0^n] \in \mathbb{R}^{n \cdot p}$ is its state vector.

The unknown function $f_0(x_0, t) : [0, \infty) \times \mathbb{R}^{n \cdot p} \to \mathbb{R}^p$ in the leader dynamics is considered to be piecewise continuous in t and locally Lipschitz in x_0, with $f_i(0, t) = 0$ for all $t \geq 0$, and all $x_0 \in \mathbb{R}^{n \cdot p}$. The governing dynamics Eqn (3) of the leader agent is private to the leader agent, and its current state value x_0 is shared only with a subset of the follower agents, serving as a reference for the formation control objectives discussed further below. The condition $f_0(0, t) = 0$ ensures that if the leader starts at the origin, it could stay there. But there is no indication that it actually does — the general form of the dynamics and the language used implies that motion is expected. Given that the leader's dynamics are general and time-varying, it serves as a formation reference. This is a dynamic tracking formation problem. The followers are expected to maintain a formation with respect to a moving leader state x_0, not converge to a fixed spatial pattern at the origin.

In the consensus problem, it is desired that

$$\lim_{t \to \infty} [(x_i^1 - \psi_i^1) - (x_0^1 - \psi_0^1)] = 0 \tag{4}$$

$$\lim_{t \to \infty} [(x_i^1 - \psi_i^1) - (x_j^1 - \psi_j^1)] = 0 \tag{5}$$

for each $i \in \mathcal{N}$ and for all $j \in \mathcal{N}$, $j \neq i$, where ψ_i^1, ψ_j^1 and $\psi_0^1 \in \mathbb{R}^p$ denote desired position offsets for agents i, j, and the leader agent 0, respectively. Following standard consensus/formation definitions (e.g., [4,20]), we adopt the desired asymptotic relations. Each agent aims to achieve a state offset from the leader or other agents by ψ_i^k, ensuring coordinated movement while maintaining formation. However, such a strong level of connectivity which requires communication among all agents is often not feasible in networked control systems due to practical constraints such as limited bandwidth, packet loss, and delays (e.g., see [18]).

The k^{th} order tracking error is defined as $\delta_i^k = (x_i^k - \psi_i^k) - (x_0^k - \psi_0^k) \in \mathbb{R}^p$, and globally as

$$\delta^k = [\delta_1^k, \delta_2^k, \ldots, \delta_N^k]^\top \in \mathbb{R}^{N \cdot p}. \tag{6}$$

Definition 2.1. *The tracking error δ^k is cooperatively uniformly ultimately bounded (CUUB) [1] if there exists a compact set $\varsigma^k \subset \mathbb{R}^{N \cdot p}$ with $\{0\} \subset \varsigma^k$ such that for any initial condition $\delta^k(t_0) \in \varsigma^k$, there exists $B^k \in \mathbb{R}_{>0}$ and $T_k \in \mathbb{R}_{>0}$ which yields $\|\delta^k(t)\| \leq B^k$ for all $t \geq t_0 + T_k$.*

In this paper, we seek a distributed consensus policy where, in addition to its own state x_i, each agent determines its input u_i based solely on the states of a limited number of other agents, which may or may not include the leader agent. Furthermore, each agent must also account for obstacle and collision avoidance.

To shape motions for collision/obstacle avoidance we employ repulsive potential terms in the spirit of [7].

Agent–agent repulsion. For $x_i^1, x_j^1 \in \mathbb{R}^p$ and $\psi_{ij}^1 > 0$,

$$m_{ij} := \begin{cases} 0, & \|x_i^1 - x_j^1\| > \psi_{ij}^1, \\ \dfrac{\varpi}{\|x_i^1 - x_j^1\|}, & \|x_i^1 - x_j^1\| \leq \psi_{ij}^1. \end{cases} \tag{7}$$

Agent–leader repulsion. For $x_0^1 \in \mathbb{R}^p$ and $\psi_{i0}^1 > 0$,

$$m_{i0} := \begin{cases} 0, & \|x_i^1 - x_0^1\| > \psi_{i0}^1, \\ \dfrac{\varpi}{\|x_i^1 - x_0^1\|}, & \|x_i^1 - x_0^1\| \le \psi_{i0}^1. \end{cases} \tag{8}$$

Agent–obstacle repulsion. Let the obstacle index set be $\mathcal{B} = \{1, \ldots, \Xi\}$, with center $O_{\mathfrak{c}} \in \mathbb{R}^p$, detection radius $R > 0$, and inner radius $\mathfrak{L} \in (0, R)$ for $\mathfrak{c} \in \mathcal{B}$. We define

$$m_{i\mathfrak{c}} := \begin{cases} 0, & \|x_i^1 - O_{\mathfrak{c}}\| > R, \\ \left[\dfrac{R^2 - \|x_i^1 - O_{\mathfrak{c}}\|^2}{\|x_i^1 - O_{\mathfrak{c}}\|^2 - \mathfrak{L}^2}\right]^2, & \mathfrak{L} < \|x_i^1 - O_{\mathfrak{c}}\| \le R. \end{cases} \tag{9}$$

The formulation for obstacle avoidance between the leader agent and obstacle is similar, with x_i^1 replaced by x_0^1.They increase as agents, the leader, or obstacles enter prescribed detection regions, thereby discouraging close approaches. In these expressions, $\varpi \in \mathbb{R}_{>0}$ is a positive scalar adjusting the repulsive force strength, $\psi_{ij}^1, \psi_{i0}^1 \in \mathbb{R}_{>0}$ are the desired scalar separation design parameters between agents i and j, and between agent i and the leader, respectively.

Let $\mathcal{G}^{\mathcal{M}} = \{\mathcal{G}^1, \ldots, \mathcal{G}^{\bar{C}}\}$ $\{\mathcal{M} = 1, \ldots, \bar{C}\}$ be a finite set of possible communication topologies, where each $\mathcal{G}^{\mathcal{M}} = (\mathcal{V}, \mathcal{E}^{\mathcal{M}}, A^{\mathcal{M}})$ is defined by; a set of agents $\mathcal{V} = \{v_1, \ldots, v_N\}$, an edge set $\mathcal{E}^{\mathcal{M}} \subseteq \mathcal{V} \times \mathcal{V}$, and an adjacency matrix $A^{\mathcal{M}}$. A piecewise constant switching signal $\sigma : \mathbb{R}_{\ge 0} \to \{1, 2, \ldots, \bar{C}\}$ governs which topology is active at time t. The signal σ is constant on each interval $[t_s, t_{s+1})$ and changes its value at $\{t_s\}$. Hence, at any $t \in [t_s, t_{s+1})$, the active topology is $\mathcal{G}^{\sigma(t)} = (\mathcal{V}, \mathcal{E}^{\sigma(t)}, A^{\sigma(t)})$. A directed edge $(v_j, v_i) \in \mathcal{E}^{\sigma(t)}$ implies that agent i can receive information from agent j. The weighted adjacency matrix $A^{\sigma(t)} = [a_{ij}^{\sigma(t)}] \in \mathbb{R}^{N \times N}$ models interaction strength under the $\sigma(t)$-th topology, where:

$$a_{ij}^{\sigma(t)} := \begin{cases} z_{w_{ij}}^{\sigma(t)} & \text{if } (v_j, v_i) \in \mathcal{E}^{\sigma(t)}, \\ 0 & \text{otherwise.} \end{cases}$$

Here, $z_{w_{ij}}^{\sigma(t)} > 0$ is the pre-defined edge weight from agent v_j to agent v_i under $\mathcal{G}^{\sigma(t)}$. The in-degree matrix for the $\sigma(t)$-th topology is $D^{\sigma(t)} = \operatorname{diag}\{d_i^{\sigma(t)}\}$ with $d_i^{\sigma(t)} = \sum_{j=1}^N a_{ij}^{\sigma(t)}$, and the corresponding Laplacian matrix is $L^{\sigma(t)} = D^{\sigma(t)} - A^{\sigma(t)}$. To incorporate a leader agent v_0, we define the augmented graph $\bar{\mathcal{G}}^{\sigma(t)} = (\bar{\mathcal{V}}, \bar{\mathcal{E}}^{\sigma(t)})$, where $\bar{\mathcal{V}} = \{v_0, v_1, \ldots, v_N\}$. The leader's influence is modeled by the diagonal matrix $B^{\sigma(t)} = \operatorname{diag}\{b_{i0}^{\sigma(t)}\}$ with $z_{w_{i0}}^{\sigma(t)} > 0$ the pre-defined edge weight from agent v_0 to agent v_i, where:

$$b_{i0}^{\sigma(t)} := \begin{cases} z_{w_{i0}}^{\sigma(t)} & \text{if } (v_0, v_i) \in \bar{\mathcal{E}}^{\sigma(t)}, \\ 0 & \text{otherwise.} \end{cases}$$

In the time-triggered switching communication topology framework, these communication links change only at a sequence of predetermined trigger instants t_s, with $t_0 = 0$ and $t_{s+1} - t_s > 0$. Between triggers the graph remains constant. If the inter-switch intervals satisfy a minimal dwell time $\tau_d > 0$, i.e. $t_{s+1} - t_s \ge \tau_d$, then σ is said to obey an average-dwell-time constraint. Thus, at any given time, the effective communication and coordination structure is defined by $\mathcal{G}^{\sigma(t)}$ (correspondingly $A^{\sigma(t)}, D^{\sigma(t)}, L^{\sigma(t)}, B^{\sigma(t)}$).

In order to ensure that no clusters of agents are isolated from the leader, we impose the following assumption.

Assumption 2.1. *Under each communication topology $\mathcal{G}^{\sigma}$, the augmented graph $\bar{\mathcal{G}}^{\sigma}$ contains a spanning tree with the leader as the root (the leader is (directly or indirectly) connected to every agent). In other words, whenever $(v_i, v_0) \notin \bar{\mathcal{E}}^{\sigma}$ under the active topology, there exists a sequence of nonzero elements of A^{σ} of the form $a_{ii_2}^{\sigma}, a_{i_2i_3}^{\sigma}, \cdots, a_{i_{l-1}i'}^{\sigma}$, for some $(i', 0) \in \bar{\mathcal{E}}^{\sigma}$, with the sequence length l being a finite integer (An agent might not communicate to the leader directly, but there is a finite hop chain of neighbors that relays leader info to it in the current graph).*

In the instantaneous-connectivity setting of [21], the communication graph is (undirected) connected at every instant, which enables arbitrarily fast switching (no dwell-time constraint) but imposes a strong per-instant topological requirement. In contrast, our framework requires leader-rooted connectivity at every instant—i.e., under Assumption 2.1 each active topology contains a spanning tree with the leader as root, so every follower is reachable (possibly through neighbors); this condition applies to both directed and undirected graphs. In addition, we enforce an average-dwell-time bound Eqn. (10) that limits the switching rate, ensuring sufficient time for information propagation and Lyapunov decrease. Thus, both approaches guarantee a per-instant connectivity property, but of different flavors and trade-offs: [21] uses all-time undirected connectivity with no timing limits, whereas we use leader-rooted connectivity plus an explicit switching-speed constraint—better capturing leader–follower networks subject to intermittent links or mobility-induced disconnections.

Due to the restrictive nature of the dwell time τ_a [19, Section 3.2.2], we employ average dwell time, τ_a^* derived in Section 4.5, that reflects the topology connectivity quality. Let $N^{\sigma}(t_0, t)$ denote the number of discontinuities of a switching signal σ on an interval (t_0, t). We say that σ has average dwell time τ_a^* [22] and [19, Section 3.2.2] if there exist two positive numbers N_0 and τ_a such that

$$N^{\sigma}(t_0, t) \le N_0 + \frac{t - t_0}{\tau_a}. \tag{10}$$

Assumption 2.1 guarantees that at every instant the leader's state is reachable by every agent via a finite neighbor chain (leader-rooted spanning tree). The average-dwell-time condition Eqn. (10) then restricts how fast we switch among such leader-connected graphs, ensuring sufficient time in each mode for information propagation and Lyapunov decrease.

Throughout the paper, we assume that the following assumptions hold.

Assumption 2.2. *The following conditions hold:*

(1) The initial states of all follower agents and the leader agent are bounded, i.e., $\|x_i(t_0)\| \le X_{\text{init}}$ for all $i \in \mathcal{N}$, and $\|x_0(t_0)\| \le X_{0,\text{init}}$, where $x_i(t_0) \in \mathbb{R}^{n \cdot p}$.

(2) There exist continuous functions $f_{\text{init}}(\cdot)$ and $f_{0,\text{init}}(\cdot)$ such that $|f_i(x)| \le |f_{\text{init}}(x)|$ for all $i \in \mathcal{N}$, and $|f_0(x_0, t)| \le |f_{0,\text{init}}(x_0)|$ for all x within the compact sets $\varsigma_f = \{x \mid \|x\| \le X_{\text{init}}\}$ and $\varsigma_0 = \{x_0 \mid \|x_0\| \le X_{0,\text{init}}\}$. These bounds hold regardless of which topology is active at any given time.

(3) The unknown disturbances $w_i(t)$ affecting each agent are bounded, i.e., $\|w(t)\| \le w_{\text{init}}$ for all $t \in [t_0, \infty)$, where $w(t) = [w_1(t); w_2(t); \ldots; w_N(t)] \in \mathbb{R}^{N \cdot p}$. This holds irrespective of the switching events and the currently active topology.

(4) The initial inter-agent, agent-leader, and agent-obstacle separations satisfy $\|x_i^1(t_0) - x_j^1(t_0)\| \ge s_{ij} > 0$, $\|x_i^1(t_0) - x_0^1(t_0)\| \ge s_{i0} > 0$, and $\|x_i^1(t_0) - O\mathfrak{c}\| \ge s_{i\mathfrak{c}} > 0$ for all $i, j \in \mathcal{N}$, $i \ne j$, $\mathfrak{c} \in \mathcal{B}$ with $0 < s_{ij} < \psi_{ij}$, $0 < s_{i0} < \psi_{i0}$ and $0 < \mathfrak{L} < s_{i\mathfrak{c}} \le R$.

To ensure that agents within a specified proximity can exchange information under the active topology, we impose the following assumption. Let $\Psi \in \mathbb{R}_{>0}$ denote a proximity threshold.

Assumption 2.3. *Under any active topology, if $\|x_i^1 - x_j^1\| \le \Psi$, then $z_{w_{ij}}^{\sigma(t)} \ne 0$.*

This assumption enforces that any pair of agents within Ψ-distance are connected by the communication graph.

3 Methodology

3.1 Neural Network Learning Problem. To account for uncertainties in the dynamics under time-triggered switching communication topologies, we use a distributed two-layer linear-in-parameters (LIP) neural network [23], enabling each agent to locally update its model as the communication graph changes. This framework allows each agent to approximate its own non-linear dynamics and those of its neighbors while sharing their states as determined by the currently active topology. Accordingly, we model the functions as:

$$f_i(x_i) = \theta_i^\top \phi_i(x_i) + \varepsilon_i, \tag{11}$$

$$f_0(x_0,t) = \theta_0^\top \phi_0(x_0,t) + \varepsilon_0, \tag{12}$$

$$w_i(t) = \theta_{iw}^\top \phi_{iw}(t) + \varepsilon_{iw}. \tag{13}$$

where $f_i(x_i) \in \mathbb{R}^p$ is the non-linear function in agent i's dynamics, $\phi_i(x_i) \in \mathbb{R}^{q_i}$, $\phi_0(x_0,t) \in \mathbb{R}^{q_0}$, and $\phi_{iw}(t) \in \mathbb{R}^{q_{iw}}$ are fixed basis functions, with the corresponding weight vectors $\theta_i \in \mathbb{R}^{p\cdot q_i}$, $\theta_0 \in \mathbb{R}^{p\cdot q_0}$, and $\theta_{iw} \in \mathbb{R}^{p\cdot q_{iw}}$, updated in real-time as new data is received from neighbors defined by the active topology. The leader's non-linear function is $f_0(x_0,t) \in \mathbb{R}^p$, and $w_i(t) \in \mathbb{R}^p$ represents the unknown disturbance affecting agent i. The approximation errors are $\varepsilon_i \in \mathbb{R}^p$, $\varepsilon_0 \in \mathbb{R}^p$, and $\varepsilon_{iw} \in \mathbb{R}^p$, q_i is the number of basis functions for agent i, q_0 is the number of basis functions for the leader agent, and q_{iw} is the number of basis functions for modeling disturbance.

The neural network approximations for $f_i(x_i)$, $f_0(x_0,t)$, and $w_i(t)$ are therefore $\hat{f}_i(x_i) = \hat{\theta}_i^\top \phi_i(x_i)$, $\hat{f}_0(x_0,t) = \hat{\theta}_0^\top \phi_0(x_0,t)$, $\hat{w}_i(t) = \hat{\theta}_{iw}^\top \phi_{iw}(t)$, where the NN weights $\hat{\theta}_i$, $\hat{\theta}_0$, and $\hat{\theta}_{iw}$ are computed locally. For brevity of notation, the basis functions and errors are denoted by

$$\theta = \mathrm{diag}(\theta_1, \ldots, \theta_N) \in \mathbb{R}^{N\cdot p \times q_t},$$

$$\phi(x) = [\phi_1^\top(x_1), \ldots, \phi_N^\top(x_N)]^\top \in \mathbb{R}^{q_t},$$

$$\varepsilon = [\varepsilon_1, \ldots, \varepsilon_N]^\top \in \mathbb{R}^{N\cdot p}.$$

Also, q_t is the total number of basis functions for all agents, $q_w = \sum_{i=1}^N q_{iw}$, and $q_t = \sum_{i=1}^N q_i$.

The global non-linearities are expressed as:

$$f(x) = \theta^\top \phi(x) + \varepsilon \tag{14}$$

$$f_0(x,t) = \theta_0^\top \phi_0(x,t) + \varepsilon_0 \tag{15}$$

$$w(t) = \theta_w^\top \phi_w(t) + \varepsilon_w \tag{16}$$

with approximations:

$$\hat{f}(x) = \hat{\theta}^\top \phi(x) \tag{17}$$

$$\hat{f}_0(x,t) = \hat{\theta}_0^\top \phi_0(x,t) \tag{18}$$

$$\hat{w}(t) = \hat{\theta}_w^\top \phi_w(t) \tag{19}$$

where $f(x) \in \mathbb{R}^{N\cdot p}$ is the concatenated non-linear function for all agents, $\theta_w = \mathrm{diag}(\theta_{1w}, \ldots, \theta_{Nw}) \in \mathbb{R}^{N\cdot p \times q_w}$, $\phi_w(t) = [\phi_{1w}(t), \phi_{2w}(t), \ldots \phi_{Nw}(t)] \in \mathbb{R}^{q_w}$, $\varepsilon_w = [\varepsilon_{1w}, \varepsilon_{2w}, \ldots, \varepsilon_{Nw}] \in \mathbb{R}^{N\cdot p}$. The NN weight errors are:

$$\tilde{\theta} = \theta - \hat{\theta}, \tag{20}$$

$$\tilde{\theta}_0 = \theta_0 - \hat{\theta}_{,0} \tag{21}$$

$$\tilde{\theta}_w = \theta_w - \hat{\theta}_w. \tag{22}$$

Assumption 3.1. *The basis functions $\phi_i(x_i)$, $\phi_0(x_0,t)$, $\phi_{iw}(t)$, the NN weights θ_i, θ_0, θ_{iw}, and the approximation errors ε, ε_0, ε_w are bounded by finite constants (not required to be known a priori)., independent of the currently active topology.*

Let $\phi_{in} = \max_{x_i\in\varsigma} \|\phi_i(x_i)\|$, $\phi_{0n} = \max_{x_0\in\varsigma, t\geq 0} \|\phi_0(x_0,t)\|$, and $\phi_{iwn} = \max_{t\geq 0}\|\phi_{iw}(t)\|$. Based on Assumption 3.1, there exist positive numbers Φ_n, Θ_n, and ε_n; Φ_{n0}, Θ_{n0}, and ε_{n0}; Φ_{nw}, Θ_{nw}, and ε_{nw}, such that: $\|\phi_i(x_i)\| \leq \Phi_n$, $\|\phi_0(x_0,t)\| \leq \Phi_{n0}$, $\|\phi_{iw}(t)\| \leq \Phi_{nw}$, $\|\theta_i\|_G \leq \Theta_n$, $\|\theta_0\|_G \leq \Theta_{n0}$, $\|\theta_{iw}\|_G \leq \Theta_{nw}$, $\|\varepsilon\| \leq \varepsilon_n$, $\|\varepsilon_0\| \leq \varepsilon_{n0}$, $\|\varepsilon_w\| \leq \varepsilon_{nw}$.

The use of a mixed dictionary of polynomial, trigonometric, and exponential basis functions is especially well-suited to adaptive control [24], since each class brings complementary approximation strengths—polynomials excel at capturing local algebraic trends, trigonometric functions model periodic behaviors, and exponentials describe transient phenomena. As demonstrated in the SINDy framework of [24], such hybrid libraries retain universal-approximation power while keeping the adaptation problem tractable: their simple, closed-form derivatives lead to well-structured, real-time optimization routines. Compared with large-scale neural networks, these basis functions yield compact adaptation laws with lower computational overhead, making them ideal for real-time control of systems with smooth nonlinearities and structured, time-varying disturbances [24].

3.2 Local Synchronization Error. With time-triggered switching communication topologies, at any given time t, the active adjacency matrix $A^{\sigma(t)}$, Laplacian $L^{\sigma(t)} = D^{\sigma(t)} - A^{\sigma(t)}$, and leader interaction matrix $B^{\sigma(t)}$ define the communication structure. Given the limited information available to the i^{th} agent under the currently active topology $\mathcal{G}^{\sigma(t)}$, we define its k^{th} order weighted synchronization error as:

$$e_i^{k,\sigma(t)} = -\nu_1 \sum_{j=1}^N a_{ij}^{\sigma(t)} \left[(x_i^k - \psi_i^k) - (x_j^k - \psi_j^k)\right] - \nu_2 b_{i0}^{\sigma(t)} \left[(x_i^k - \psi_i^k) - (x_0^k - \psi_0^k)\right], \tag{23}$$

where $\nu_1, \nu_2 > 0$ are scalar gains, $a_{ij}^{\sigma(t)}$ are the entries of the active adjacency matrix $A^{\sigma(t)}$, and $b_{i0}^{\sigma(t)}$ are the entries of the leader interaction matrix $B^{\sigma(t)}$. For notational convenience, we employ $e_i^{k,\sigma(t)}$ and e_i^k interchangeably throughout the manuscript to represent the same mathematical entity. The scalar gains ν_1, ν_2 can vary between topologies, however, in this paper, we consider them constant across topologies. Using the simplifying notations: $\bar{x}_i^k := x_i^k - \psi_i^k$, $\bar{x}_j^k := x_j^k - \psi_j^k$ and $\bar{x}_0^k := x_0^k - \psi_0^k$, we rewrite Eqn. (23) as:

$$e_i^{k,\sigma(t)} = -\nu_1 \sum_{j=1}^N a_{ij}^{\sigma(t)} (\bar{x}_i^k - \bar{x}_j^k) - \nu_2 b_{i0}^{\sigma(t)} (\bar{x}_i^k - \bar{x}_0^k). \tag{24}$$

Here, the term $-\nu_1 \sum_{j=1}^N a_{ij}^{\sigma(t)} (\bar{x}_i^k - \bar{x}_j^k)$ ensures consensus among agents by penalizing the difference between the state of agent i and its neighbors, while $-\nu_2 b_{i0}^{\sigma(t)} (\bar{x}_i^k - \bar{x}_0^k)$ couples the agent's state to the leader state by penalizing their difference. Defining, $e^{k,\sigma(t)} = [e_1^{k,\sigma(t)}, e_2^{k,\sigma(t)}, e_3^{k,\sigma(t)}, \ldots, e_N^{k,\sigma(t)}]^\top \in \mathbb{R}^{N\cdot p}$, $\underline{\bar{x}}_0^k = [\bar{x}_0^k, \ldots, \bar{x}_0^k]^\top \in \mathbb{R}^{N\cdot p}$, $\bar{x}^k = [\bar{x}_1^k, \ldots, \bar{x}_N^k]^\top \in \mathbb{R}^{N\cdot p}$, we reformulate Eqn. (24) in global form as:

$$e^{k,\sigma(t)} = -(\nu_1 L^{\sigma(t)} + \nu_2 B^{\sigma(t)})(\bar{x}^k - \underline{\bar{x}}_0^k), \tag{25}$$

highlighting that the synchronization error depends on the currently active topology.

Lemma 1. *Under Assumption 2.1, the matrices* $\nu_1 L^{\sigma(t)} + \nu_2 B^{\sigma(t)}$ *are non-singular for all topologies* $\sigma(t)$.

Proof. Let J denote the set of strictly diagonally dominant nodes of $\mathscr{S}^{\sigma(t)} := \nu_1 L^{\sigma(t)} + \nu_2 B^{\sigma(t)}$, i.e, $J = \{i : |\mathscr{S}_{ii}^{\sigma(t)}| > \sum_{j \neq i} |\mathscr{S}_{ij}^{\sigma(t)}|\}$. Similar to the proof under a fixed topology, if $J = \mathcal{N}$, i.e., the matrix $\mathscr{S}^{\sigma(t)}$ is strictly diagonally dominant, then $\det(\mathscr{S}^{\sigma(t)}) \neq 0$ is directly obtained by the application of the Gershgorin circle theorem [25]. For the case where $J \subset \mathcal{N}$ is a strict subset of agents, we note from $\mathscr{S}^{\sigma(t)} := \nu_1 L^{\sigma(t)} + \nu_2 B^{\sigma(t)}$ and $L^{\sigma(t)} := D^{\sigma(t)} - A^{\sigma(t)}$ that $\mathscr{S}^{\sigma(t)} = \nu_1 D^{\sigma(t)} - \nu_1 A^{\sigma(t)} + \nu_2 B^{\sigma(t)}$. Since $B^{\sigma(t)} := \mathrm{diag}\{b_i^0\}$ and $D := \mathrm{diag}\{d_i^{\sigma(t)}\}$ are diagonal matrices, the on-diagonal elements of $\mathscr{S}^{\sigma(t)}$ are $\mathscr{S}_{ii}^{\sigma(t)} = -\nu_1 d_{ii} - \nu_2 b_i^0$ and the off-diagonal elements are $\mathscr{S}_{ij}^{\sigma(t)} = -\nu_1 a_{ij}$, $i \neq j$. These relations, together with Assumption 2.1, yields that: (i) $J \neq \emptyset$ and (ii) for each agent $i \notin J$, there exists a sequence of nonzero elements of $\mathscr{S}^{\sigma(t)}$ in the form $\mathscr{S}_{i_1 i_2}, \mathscr{S}_{i_2 i_3}, \ldots, \mathscr{S}_{i_{s-1} i_s}$, for some $i_s \in J$, which directly correspond to the sequence of non-zero elements $a_{i_1 i_2}, a_{i_2 i_3}, \ldots, a_{i_{s-1} i_s}$ in Assumption 2.1 (applied to each active topology $\mathcal{G}^{\sigma(t)}$). Thus, by invoking [26, Theorem], we conclude that $\mathscr{S}^{\sigma(t)}$ is non-singular under any active topology. □

3.3 Local Error Dynamics. Under time-triggered switching communication topologies, the active Laplacian and leader-interaction matrices at time t are $L^{\sigma(t)}$ and $B^{\sigma(t)}$. For each time t, the differentiation of the synchronization error defined in Eqn. (24) yields:

$$\dot{e}^{k,\sigma(t)} = e^{k+1,\sigma(t)}, \quad k = 1, \ldots, n-1$$
$$\dot{e}^{k,\sigma(t)} = -(\nu_1 L^{\sigma(t)} + \nu_2 B^{\sigma(t)})(\dot{\bar{x}}^n - \dot{\underline{\bar{x}}}_0^n), \quad k = n \tag{26}$$

which, in the expanded form, is written as:

$$\dot{e}^1 = e^2 = -(\nu_1 L^{\sigma(t)} + \nu_2 B^{\sigma(t)})(\bar{x}^2 - \underline{\bar{x}}_0^2)$$
$$\dot{e}^2 = e^3 = -(\nu_1 L^{\sigma(t)} + \nu_2 B^{\sigma(t)})(\bar{x}^3 - \underline{\bar{x}}_0^3)$$
$$\vdots$$
$$\dot{e}^n = -(\nu_1 L^{\sigma(t)} + \nu_2 B^{\sigma(t)})(f(\bar{x}) + u + w - f_0(\bar{x}_0, t)) \tag{27}$$

where $e^{k,\sigma(t)} \in \mathbb{R}^{N \cdot p}$, $\bar{x}^k \in \mathbb{R}^{N \cdot p}$, and $\underline{\bar{x}}_0^k \in \mathbb{R}^{N \cdot p}$. Here, $f(\bar{x})$, $f_0(\bar{x}_0, t)$, u, and w represent the aggregated nonlinearities, leader dynamics, control input, and disturbances, respectively, and evolve under the currently active communication topology defined by $\sigma(t)$.

3.4 Weighted Stability Error. The weighted stability error $r_i \in \mathbb{R}^p$ for each follower agent i is defined as:

$$\begin{aligned} r_i &= \lambda_1 e_i^1 + \lambda_2 e_i^2 + \cdots + \lambda_{n-1} e_i^{n-1} + e_i^n \\ &= -\nu_1 \sum_{k=1}^{n} \sum_{j=1}^{N} \lambda_k a_{ij}^{\sigma(t)} \left[(x_i^k - \psi_i^k) - (x_j^k - \psi_j^k) \right] \\ &\quad - \nu_2 \sum_{k=1}^{n} \lambda_k b_{i0}^{\sigma(t)} \left[(x_i^k - \psi_i^k) - (x_0^k - \psi_0^k) \right] \end{aligned} \tag{28}$$

with $\lambda_n = 1$, and where λ_j (for $j = 1, \ldots, n-1$) the design parameters are chosen such that the characteristic polynomial:

$$\mathfrak{s}^{n-1} + \lambda_{n-1} \mathfrak{s}^{n-2} + \cdots + \lambda_1 \tag{29}$$

is Hurwitz. This ensures that all roots have negative real parts, leading to the stability of the associated linear system. The selection of λ_j can be made by setting $\mathfrak{s}^{n-1} + \lambda_{n-1}\mathfrak{s}^{n-2} + \cdots + \lambda_1 = \prod_{j=1}^{n-1}(\mathfrak{s} - \xi_j)$, and selecting ξ_j's to be positive real numbers. The global form of the representation of the weighted stability error is:

$$r = \lambda_1 e^1 + \lambda_2 e^2 + \cdots + \lambda_{n-1} e^{n-1} + e^n \in \mathbb{R}^{N \cdot p \times 1}. \tag{30}$$

Similarly, we define

$$\begin{aligned} \rho_i &= \lambda_1 e_i^2 + \lambda_2 e_i^3 + \cdots + \lambda_{n-1} e_i^n \\ &= -\nu_1 \sum_{k=2}^{n} \sum_{j=1}^{N} \lambda_{k-1} a_{ij}^{\sigma(t)} \left[(x_i^k - \psi_i^k) - (x_j^k - \psi_j^k) \right] \\ &\quad - \nu_2 \sum_{k=2}^{n} \lambda_{k-1} b_{i0}^{\sigma(t)} \left[(x_i^k - \psi_i^k) - (x_0^k - \psi_0^k) \right] \end{aligned} \tag{31}$$

as well as

$$\rho = \lambda_1 e^2 + \lambda_2 e^3 + \lambda_3 e^4 + \cdots + \lambda_{n-1} e^n. \tag{32}$$

By differentiating Eqn. (30) with respect to time, the weighted stability error dynamics under the active topology $\sigma(t)$ is written as:

$$\begin{aligned} \dot{r} &= \lambda_1 \dot{e}^1 + \lambda_2 \dot{e}^2 + \cdots + \lambda_{n-1} \dot{e}^{n-1} + \dot{e}^n \\ &= \lambda_1 e^2 + \lambda_2 e^3 + \cdots + \lambda_{n-1} e^n \\ &\quad - (\nu_1 L^{\sigma(t)} + \nu_2 B^{\sigma(t)})(\dot{\bar{x}}^n - \dot{\underline{\bar{x}}}_0^n) \end{aligned}$$

recalling from Eqn. (26) that $\dot{e}^n = -(\nu_1 L^{\sigma(t)} + \nu_2 B^{\sigma(t)})(\dot{\bar{x}}^n - \dot{\underline{\bar{x}}}_0^n)$. Hence, $\dot{r}$ can be written as

$$\dot{r} = \rho - (\nu_1 L^{\sigma(t)} + \nu_2 B^{\sigma(t)})(f(x) + u + w - f_0(x_0, t)), \tag{33}$$

where

$$\bar{\lambda} = [\lambda_1, \lambda_2, \ldots, \lambda_{n-1}]^\top \tag{34}$$

With the definition of $E_1 = [e^1, e^2, \ldots, e^{n-1}] \in \mathbb{R}^{N \cdot p \times (n-1)}$, and $E_2 = [e^2, e^3, \ldots, e^n] \in \mathbb{R}^{N \cdot p \times (n-1)}$, we first rewrite (32) as $\rho = E_2 \bar{\lambda}$ and, further, we can write the matrix relation:

$$E_2 = E_1 \triangle^\top + r\, l = \dot{E}_1 = [e^2, e^3, \ldots, e^n] \in \mathbb{R}^{1 \times N \cdot p \cdot (n-1)} \tag{35}$$

with $l = [0, 0, \ldots, 0, 1] \in \mathbb{R}^{1 \times (n-1)}$, and

$$\triangle = \begin{bmatrix} 0 & 1 & 0 & \ldots & 0 \\ 0 & 0 & 1 & \ldots & 0 \\ \vdots & \vdots & \vdots & \ddots & \vdots \\ 0 & 0 & 0 & \ldots & 1 \\ -\lambda_1 & -\lambda_2 & -\lambda_3 & \ldots & -\lambda_{n-1} \end{bmatrix} \in \mathbb{R}^{(n-1) \times (n-1)}.$$

As stated in [1], since $\triangle$ is Hurwitz, there exists a unique positive-definite matrix $P_1^{\sigma(t)}$ such that for any positive number β:

$$\triangle^\top P_1^{\sigma(t)} + P_1^{\sigma(t)} \triangle = -\beta I \tag{36}$$

where $I \in \mathbb{R}^{(n-1) \times (n-1)}$ is the identity matrix. We will use $P_1^{\sigma(t)}$ in the Lyapunov function to establish convergence.

Lemma 2. *If* $r_i(t)$ *is ultimately bounded, then* $e_i(t)$ *is ultimately bounded.*

Proof. The result is direct consequence of [1, Lemma 10.3]. □

Lemma 3 (Graph Lyapunov Equation)**.** *Define*

$$q \equiv [q_1, \dots, q_N]^\top := (\nu_1 L^{\sigma(t)} + \nu_2 B^{\sigma(t)})^{-1} \underline{1}, \tag{37}$$

$$P^{\sigma(t)} := diag\{1/q_i\}_{i\in\mathcal{N}}, \tag{38}$$

$$Q^{\sigma(t)} := P^{\sigma(t)}(\nu_1 L^{\sigma(t)} + \nu_2 B^{\sigma(t)}) + (\nu_1 L^{\sigma(t)} + \nu_2 B^{\sigma(t)})^\top P^{\sigma(t)}, \tag{39}$$

where $\underline{1} = [1, \dots, 1]^\top \in \mathbb{R}^N$. *Then the matrices* $P^{\sigma(t)}$ *and* $Q^{\sigma(t)}$ *are positive definite.*

Proof. The proof is similar to [1, Lemma 10.1] by arguing that $\nu_1 L^{\sigma(t)} + \nu_2 B^{\sigma(t)}$ is non-singular by Lemma 1. □

4 Main Result

We now introduce the proposed distributed control strategy and adaptive tuning laws in Sections 4.1 and 4.3, respectively.

4.1 Proposed distributed Control Law.

Under time-triggered switching communication topologies, let $D^{\sigma(t)}$ and $B^{\sigma(t)}$ be the in-degree and leader-interaction matrices corresponding to the active topology $\sigma(t)$. Given, $c_i \in \mathbb{R}^{p\times np}$ a tunable gain matrix and

$$E_{i0} = \begin{bmatrix} (x_i^1 - \psi_i^1) - (x_0^1 - \psi_0^1) \\ \vdots \\ (x_i^k - \psi_i^k) - (x_0^k - \psi_0^k) \\ \vdots \\ (x_i^n - \psi_i^n) - (x_0^n - \psi_0^n) \end{bmatrix} \tag{40}$$

is the relative position between the follower and leader with global forms represented as c and E_0, respectively. To achieve a fully modular design that simultaneously handles formation tracking, disturbance rejection, consensus, leader-following, and safety, our control law for high-dimensional nonlinear agent i is composed of five clear components. First, the feedforward term ρ_i encodes the desired leader-follower offset ψ_i^k, ensuring each agent follows the leader (ψ_i^1 is the relative displacement). Second, the adaptive neural-network terms $-\hat{\theta}_i^\top \phi_i - \hat{\theta}_{iw}^\top \phi_{iw} + \hat{\theta}_0^\top \phi_0$ cancel unknown agent dynamics and external disturbances via online weight adaptation. Third, the synchronization error r_i drives all inter-agent and agent-leader deviations—after subtracting offset thresholds—to zero, enforcing cohesion. Fourth, a proportional leader-tracking correction $-c_i E_{i0}^\top$ guarantees exponential convergence to the leader's trajectory through the communication graph. Finally, the repulsive safety forces $\Gamma_\mathfrak{c}^0 \sum_{\mathfrak{c}=1}^{\xi} m_{i\mathfrak{c}}\, n_{i\mathfrak{c}}, \Gamma_{ij}^1 \sum_{j=1}^N m_{ij}\, n_{ij}, \Gamma_{i0}^2 \sum_{j=1}^N m_{i0}\, n_{i0}$ provide proximity-dependent safety shaping by pushing agents away from nearby hazards.

Each term directly maps to one of our core objectives, resulting in a tunable control architecture. The proposed distributed control law is presented for each agent i as:

$$u_i = \frac{\rho_i}{d_i^{\sigma(t)} + b_{i0}^{\sigma(t)}} - \hat{\theta}_i^\top \phi_i - \hat{\theta}_{iw}^\top \phi_{iw} + \hat{\theta}_0^\top \phi_0 + r_i - c_i E_{i0}^\top + \sum_{\mathfrak{c}=1}^{\Xi} \Gamma_\mathfrak{c}^0 m_{i\mathfrak{c}} n_{i\mathfrak{c}} + \Gamma_{ij}^1 m_{ij}\, n_{ij} + \Gamma_{i0}^2 \sum_{j=1}^N m_{i0}\, n_{i0} \tag{41}$$

where

$$n_{ij} := \frac{x_i^1 - x_j^1}{\|x_i^1 - x_j^1\|}, \qquad n_{i0} := \frac{x_i^1 - x_0^1}{\|x_i^1 - x_0^1\|}, \qquad n_{i\mathfrak{c}} := \frac{x_i^1 - O_\mathfrak{c}}{\|x_i^1 - O_\mathfrak{c}\|}. \tag{42}$$

i.e., the repulsive inputs in Eqn. (7)–(9) act along the line-of-centers between agent i and agent j, agent i and the leader, and agent i and obstacle $\mathfrak{c}$, respectively. The control law (42) is written in expanded form as

$$\begin{aligned} u_i = \frac{1}{d_i^{\sigma(t)} + b_{i0}^{\sigma(t)}} \Bigg(&- \nu_1 \sum_{k=2}^{n} \sum_{j=1}^{N} \lambda_{k-1} a_{ij}^{\sigma(t)} \Big[(x_i^k - \psi_i^k) - (x_j^k - \psi_j^k) \Big] - \nu_2 \sum_{k=2}^{n} \lambda_{k-1} b_{i0}^{\sigma(t)} \Big[(x_i^k - \psi_i^k) - (x_0^k - \psi_0^k) \Big] \Bigg) \\ &- \hat{\theta}_i^\top \phi_i(x_i) - \hat{\theta}_{iw}^\top \phi_{iw}(t) + \hat{\theta}_0^\top \phi_0(x_0, t) - \nu_1 \sum_{k=1}^{n} \sum_{j=1}^{N} \lambda_k a_{ij}^{\sigma(t)} \Big[(x_i^k - \psi_i^k) - (x_j^k - \psi_j^k) \Big] \\ &- \nu_2 \sum_{k=1}^{n} \lambda_k b_{i0}^{\sigma(t)} \Big[(x_i^k - \psi_i^k) - (x_0^k - \psi_0^k) \Big] - \sum_{k=1}^{n} c_i^k \Big[(x_i^k - \psi_i^k) - (x_0^k - \psi_0^k) \Big] \\ &+ \sum_{\mathfrak{c}=1}^{\Xi} \Gamma_\mathfrak{c}^0\, m_{i\mathfrak{c}}(x_i, O_\mathfrak{c})\, n_{i\mathfrak{c}} + \sum_{j=1}^{N} \Gamma_{ij}^1\, m_{ij}(x_i, x_j)\, n_{ij} + \Gamma_{i0}^2\, m_{i0}(x_i, x_0)\, n_{i0}. \end{aligned} \tag{43}$$

To facilitate the discussion, Eqn. (41) is decomposed as

$$u_i^d = \frac{\rho}{d_i^{\sigma(t)} + b_{i0}^{\sigma(t)}} - \hat{\theta}_i^\top \phi_i - \hat{\theta}_{iw}^\top \phi_{iw} + \hat{\theta}_0^\top \phi_0 + r_i - c_i E_{i0}^\top, \tag{44}$$

$$u_i^0 = \Gamma_\mathfrak{c}^0 \sum_{\mathfrak{c}=1}^{\xi} m_{i\mathfrak{c}} n_{i\mathfrak{c}}, \tag{45}$$

$$u_i^c = \Gamma_{ij}^1 \sum_{j=1}^{N} m_{ij} n_{ij} + \Gamma_{i0}^2 \sum_{j=1}^{N} m_{i0} n_{i0}. \tag{46}$$

This yields the global form of the control law U as:

$$U = U^d + U^0 + U^c \tag{47}$$

where:

$$U^d = (D^{\sigma(t)} + B^{\sigma(t)})^{-1} \rho - \hat{\theta}^\top \phi - \hat{\theta}_w^\top \phi_w + \hat{\theta}_0^\top \phi_0 + r - c E_0^\top, \tag{48}$$

$$U^0 = \Gamma^0 M^0, \tag{49}$$

$$U^c = \Gamma^1 M_I^c + \Gamma^2 M_0^c. \tag{50}$$

Gain matrices $\Gamma^0, \Gamma^1, \Gamma^2$ multiply the obstacle-avoidance term M^0 and the two collision-avoidance terms M_I^c, M_0^c. Each Γ^j is a constant, positive-definite matrix chosen by the designer to set the relative priority and shape of those repulsive contributions. The overall control law is:

$$U = (D^{\sigma(t)} + B^{\sigma(t)})^{-1}\rho - \hat{\theta}^\top \phi - \hat{\theta}_w^\top \phi_w + \hat{\theta}_0^\top \phi_0$$
$$+ r - cE_0^\top + \Gamma^0 M^0 + \Gamma^1 M_I^c + \Gamma^2 M_0^c \tag{51}$$

Here, $U = [u_1^\top, u_2^\top, \ldots, u_N^\top]^\top \in \mathbb{R}^{N \cdot p}$ is the control input vector for all agents with $u_i, u_i^d, u_i^c, u_i^0 \in \mathbb{R}^p$, and $(D^{\sigma(t)} + B^{\sigma(t)})^{-1}$ is the inverse of the diagonal matrix $\text{diag}[(d_1^{\sigma(t)} + b_{10}^{\sigma(t)})I_p, (d_2^{\sigma(t)} + b_{20}^{\sigma(t)})I_p, \ldots, (d_N^{\sigma(t)} + b_{N0}^{\sigma(t)})I_p] \in \mathbb{R}^{(N\cdot p)\times(N\cdot p)}$. I_p is the identity matrix of size $p \times p$. The global neural network weight matrices $\hat{\theta}, \hat{\theta}_w, \hat{\theta}_0$ correspond to the agents' dynamics, disturbances, and leader's dynamics, while the global basis function matrices ϕ, ϕ_w, ϕ_0 relate to these respective dynamics. The control law U thus adapts to the currently active topology $\sigma(t)$, ensuring performance and stability despite the evolving communication structure.

4.2 Boundedness of the Control Input.

Proposition 4.1. *For a system with follower dynamics (1) and leader dynamics (3) with $n \geq 3$, and under Assumptions 2.2(1), Assumptions 2.2(3), Assumptions 2.2(4) and 3.1, the control law (41) generates a bounded input under the admissible switching communication topology. That is, there exists a constant $u_n < \infty$ such that $\|u(t)\| \leq u_n$, $\forall t \geq t_0$.*

Proof. The use of repulsive components in the input (41) renders the collision configurations

$$x_{ij}^{\text{col}} := \left\{ [x_1^\top \cdots x_N^\top]^\top \in \mathbb{R}^{Nnp} \,\middle|\, x_i^1 - x_j^1 = 0 \right\}$$

(and similarly the obstacle–collision configurations) unstable. In particular, one can construct Chetaev functions V_{ij}^{col} (and their obstacle counterparts) that are positive in a neighborhood of these sets and satisfy $\dot{V}_{ij}^{\text{col}} > 0$. Hence, under Assumption 2.2(4) and the proposed control law, one can construct level sets of $V_{ij}^{\text{col}} > 0$ such that

$$m_{ij}(t) \leq M_{ij}, \quad m_{i0}(t) \leq M_{i0}, \quad m_{i\mathfrak{c}}(t) \leq M_{i\mathfrak{c}}, \quad \forall t \geq t_0.$$

In other words, the repulsive components satisfy

$$\|u_i^0(t)\| \leq \sum_{\mathfrak{c}=1}^{\Xi} \|\Gamma_{\mathfrak{c}}^0\|\, M_{i\mathfrak{c}} < \infty,$$

and

$$\|u_i^c(t)\| \leq \sum_{j=1}^{N} \|\Gamma_{ij}^1\|\, M_{ij} + \|\Gamma_{i0}^2\|\, M_{i0} < \infty.$$

For the non-repulsive part u_i^d, Assumption 3.1 ensures that all basis functions, NN weights, and approximation errors are bounded. Moreover, by Theorem 4.1, the closed-loop signals are bounded and the tracking/synchronization errors are ultimately bounded; in particular, r_i and E_{i0} remain bounded for all $t \geq t_0$. Also, by Assumption 2.1, there exists $\underline{d} > 0$ such that

$$d_i^{\sigma(t)} + b_{i0}^{\sigma(t)} \geq \underline{d} \quad \Rightarrow \quad (d_i^{\sigma(t)} + b_{i0}^{\sigma(t)})^{-1} \leq \underline{d}^{-1}.$$

Hence every term in u_i^d is uniformly bounded, and therefore $\|u_i^d(t)\|$ is uniformly bounded.

Since $u_i = u_i^d + u_i^0 + u_i^c$, each component of u_i is bounded, therefore there exists $u_{i,n} < \infty$ such that

$$\|u_i(t)\| \leq u_{i,n}, \qquad \forall t \geq t_0.$$

Stacking over all agents yields

$$\|u(t)\| \leq u_n$$

for some finite constant $u_n < \infty$ and all $t \geq t_0$. Because the admissible switching signal takes values in a finite family of communication topologies, the above bound is uniform across topology switches. □

It is worth remarking that the bound u_n depends on multiple parameters, particularly the potential functions bounds from Assumption 2.2(4), the NN weight and basis-function bounds from Assumption 3.1, the closed-loop error bounds from Theorem 4.1, and the minimum sum of the in-degree and leader-coupling $\underline{d} = \min_{i,\sigma}(d_i^\sigma + b_{i0}^\sigma)$ from Assumption 2.1. Consequently, while the large number of variables makes an explicit closed-form calculation impractical, Proposition 4.1 establishes the existence of such finite upper bound u_n that is strictly determined by the system bounds and design parameters.

4.3 Proposed NN Local Tuning Laws. At any time t, the active topology $\sigma(t)$ determines the in-degree matrix $D^{\sigma(t)}$ and the leader-interaction matrix $B^{\sigma(t)}$. For each agent i, the NN parameter adaptive tuning laws are proposed as:

$$\dot{\hat{\theta}}_i = -G_i\left[\phi_i r_i p_i (d_i^{\sigma(t)} + b_{i0}^{\sigma(t)}) + \kappa_i \hat{\theta}_i\right], \tag{52}$$

$$\dot{\hat{\theta}}_0 = G_{i0}\left[\phi_0 r_i p_i (d_i^{\sigma(t)} + b_{i0}^{\sigma(t)}) - \kappa_0 \hat{\theta}_0\right], \tag{53}$$

$$\dot{\hat{\theta}}_{iw} = -G_{iw}\left[\phi_{iw} r_i p_i (d_i^{\sigma(t)} + b_{i0}^{\sigma(t)}) + \kappa_{iw} \hat{\theta}_{iw}\right]. \tag{54}$$

where, $\kappa_i, \kappa_0, \kappa_{iw} \in \mathbb{R}_{>0}$ are positive scalar tuning gains. Here $G_i \in \mathbb{R}^{q_i \times q_i}$, $G_{i0} \in \mathbb{R}^{q_0 \times q_0}$, and $G_{iw} \in \mathbb{R}^{q_{iw} \times q_{iw}}$ are constant, symmetric positive–definite matrices that serve as the adaptation-rate (gain) matrices for the agent–dynamics, leader–dynamics and disturbance neural networks respectively. Their magnitudes can be tuned to trade off convergence speed versus robustness to noise or unmodelled dynamics. In the global context, this yields the parameter estimate dynamics as:

$$\dot{\hat{\theta}} = -G\left[\phi r^\top P^{\sigma(t)}(D^{\sigma(t)} + B^{\sigma(t)}) + \kappa \hat{\theta}\right], \tag{55}$$

$$\dot{\hat{\theta}}_0 = G_0^*\left[\phi_0 r^\top P^{\sigma(t)}(D^{\sigma(t)} + B^{\sigma(t)}) - \kappa_0 \hat{\theta}_0\right], \tag{56}$$

$$\dot{\hat{\theta}}_w = -G_w\left[\phi_w r^\top P^{\sigma(t)}(D^{\sigma(t)} + B^{\sigma(t)}) + \kappa_w \hat{\theta}_w\right]. \tag{57}$$

where

$$G = \text{diag}(G_1, \ldots, G_N) \in \mathbb{R}^{q_t \times q_t},$$

$$G_0^* = \text{diag}(G_0, \ldots, G_0) \in \mathbb{R}^{q_t \times q_t},$$

$$G_w = \text{diag}(G_{1w}, \ldots, G_{Nw}) \in \mathbb{R}^{q_t \times q_t}.$$

The matrix $P^{\sigma(t)}$ is defined as in Eqn. (38), and κ, κ_0, and κ_w are vectors of the tuning gains $\kappa_i, \kappa_0, \kappa_{iw}$ respectively.

4.4 Leader-Follower Formation Consensus.

Theorem 4.1. *For the distributed multi-agent with the follower dynamics Eqn. (1) and leader dynamics Eqn. (3) under assumptions 2.2, 2.1, and 3.1, the NN tuning laws Eqn. (53), Eqn. (52), Eqn. (54), together with the control law Eqn. (41), and for a network satisfying the average dwell-time condition Eqn. (81) later derived in Proposition 4.2, this results in synchronization, collision and obstacle avoidance, and global asymptotic stability under switching communication topology in the form of*

(1) Synchronization: The tracking errors, δ^k in Eqn. (6), for all follower agents, $i \in \mathcal{N}$ are cooperatively uniformly ultimately bounded (CUUB).
(2) Stability: The origin is globally stable for all the k^{th} order weighted synchronization errors Eqn. (23), i.e., $e_i^{k,\sigma(t)}$ for all $k \in \{1, \cdots, n\}$, $i \in \{1, \cdots, N\}$, the weighted stability error Eqn. (30), and the NN weight errors $\tilde{\theta} = \theta - \hat{\theta}$, $\tilde{\theta}_0 = \theta_0 - \hat{\theta}_0$, $\tilde{\theta}_w = \theta_w - \hat{\theta}_w$.
(3) Collision and Obstacle Avoidance: Agents avoid collisions and obstacles while maintaining synchronization and stability, i.e., $m_{ij}n_{ij}$ in Eqn. (7), $m_{i0}n_{i0}$ in Eqn. (8), and $m_{ic}n_{ic}$ in Eqn. (9) combined with Eqn. (42) for all $t \geq 0$.

The CUUB/weight bounds are existential (used for analysis); implementation does not require numerical knowledge of these constants. Boundedness of $\hat{\theta}$, $\hat{\theta}_0$ and $\hat{\theta}_w$ are enforced by the terms in the NN local tuning laws.

Proof. **Part 1:** For a high-order, high-dimensional, nonlinear, heterogeneous multi-agent system, we extend the Lyapunov-derivative summation and norm-bounding methodology of [1] to accommodate time-triggered switching communication topologies, collision and obstacle avoidance, and online disturbance estimation via adaptive neural networks. We consider the Lyapunov function:

$$V^\sigma = V_1^\sigma + V_2^\sigma + V_3^\sigma + V_4^\sigma + V_5^\sigma \tag{58}$$

with each term defined to capture the dynamics, NN weight errors, and synchronization errors under the active topology. Specifically $V_1^\sigma = \frac{1}{2} r^\top P^{\sigma(t)} r$, $V_2^\sigma = \frac{1}{2}\mathrm{tr}\{\tilde{\theta}^\top G^{-1}\tilde{\theta}\}$, $V_3^\sigma = \frac{1}{2}\mathrm{tr}\{\tilde{\theta}_0^\top G_0^{*-1}\tilde{\theta}_0\}$, $V_4^\sigma = \frac{1}{2}\mathrm{tr}\{\tilde{\theta}_w^\top G_w^{-1}\tilde{\theta}_w\}$, and $V_5^\sigma = \frac{1}{2}\mathrm{tr}\{E_1 P_1^{\sigma(t)}(E_1)^\top\}$. Taking the derivative of V_1^σ and using Eqn. (33), yields

$$\dot{V}_1^\sigma = r^\top P^{\sigma(t)}\dot{r} = r^\top P^{\sigma(t)}\Big[\rho - (\nu_1 L^{\sigma(t)} + \nu_2 B^{\sigma(t)})(f(x) + u + w - f_0(x_0, t))\Big].$$

Substituting Eqn. (47), we have

$$\dot{V}_1^\sigma = r^\top P^{\sigma(t)}\Big[\rho - (\nu_1 L^{\sigma(t)} + \nu_2 B^{\sigma(t)})[f + (D^{\sigma(t)} + B^{\sigma(t)})^{-1}\rho - \hat{\theta}^\top\phi - \hat{\theta}_w^\top\phi_w + \hat{\theta}_0^\top\phi_0 + r - cE_0^\top + \Gamma^0 M^0 + \Gamma^1 M_I^c + \Gamma^2 M_0^c + w - f_0]\Big]. \tag{59}$$

Considering Eqn. (14) through Eqn. (19), Eqn. (39) and invoking the property $a^\top b = \mathrm{tr}\{b\, a^\top\}$ after further simplification, we obtain $\dot{V}_1^\sigma$ as

$$\begin{aligned}\dot{V}_1^\sigma &= -\frac{1}{2} r^\top Q^{\sigma(t)} r - \mathrm{tr}\{\tilde{\theta}^\top\phi r^\top P^{\sigma(t)}(D^{\sigma(t)} + B^{\sigma(t)})\}\\ &+ \mathrm{tr}\{\tilde{\theta}^\top\phi r^\top P^{\sigma(t)} A^{\sigma(t)}\} - \mathrm{tr}\{\tilde{\theta}_w^\top\phi_w r^\top P^{\sigma(t)}(D^{\sigma(t)} + B^{\sigma(t)})\}\\ &+ r^\top P^{\sigma(t)} A^{\sigma(t)}(D^{\sigma(t)} + B^{\sigma(t)})^{-1}\rho + \frac{1}{2} c r^\top Q^{\sigma(t)} E_0^\top\\ &+ \mathrm{tr}\{\tilde{\theta}_w^\top\phi_w r^\top P^{\sigma(t)} A^{\sigma(t)}\} + \mathrm{tr}\{\tilde{\theta}_0^\top\phi_0 r^\top P^{\sigma(t)}(D^{\sigma(t)} + B^{\sigma(t)})\}\\ &- \mathrm{tr}\{\tilde{\theta}_0^\top\phi_0 r^\top P^{\sigma(t)} A^{\sigma(t)}\}\\ &- r^\top P^{\sigma(t)}(\nu_1 L^{\sigma(t)} + \nu_2 B^{\sigma(t)})(\varepsilon + \epsilon_w - \epsilon_0)\\ &+ r^\top P^{\sigma(t)}(\nu_1 L^{\sigma(t)} + \nu_2 B^{\sigma(t)})(\Gamma^0 M^0 + \Gamma^1 M_I^c + \Gamma^2 M_0^c).\end{aligned} \tag{60}$$

Differentiating V_2^σ with respect to time results in

$$\dot{V}_2^\sigma = tr\{\tilde{\theta}^\top G^{-1}\dot{\tilde{\theta}}\}. \tag{61}$$

Differentiating Eqn. (20) and substituting $\dot{\tilde{\theta}} = -\dot{\hat{\theta}}$ yields:

$$\dot{V}_2^\sigma = -tr\{\tilde{\theta}^\top G^{-1}\dot{\hat{\theta}}\}, \tag{62}$$

Likewise, differentiating Eqn. (21) and Eqn. (22) yields:

$$\dot{V}_3^\sigma = -tr\{\tilde{\theta}_0^\top G_0^{*-1}\dot{\hat{\theta}}_0\}, \tag{63}$$

$$\dot{V}_4^\sigma = -tr\{\tilde{\theta}_w^\top G_w^{-1}\dot{\hat{\theta}}_w\}. \tag{64}$$

The derivative of V_5^σ is $\dot{V}_5^\sigma = tr\{\dot{E}_1 P_1^{\sigma(t)}(E_1)^\top\}$. Using Eqn. (35), then, $\dot{V}_5^\sigma = \frac{1}{2} tr\{E_1(\triangle^\top P_1^{\sigma(t)} + P_1^{\sigma(t)}\triangle)(E_1)^\top\} + tr\{rl^\top P_1^{\sigma(t)}(E_1)^\top\}$. Considering Eqn. (36), $\dot{V}_5^\sigma$ becomes

$$\dot{V}_5^\sigma = -\frac{\beta}{2}||E_1||_G^2 + \bar{\alpha}(P_1^{\sigma(t)})||l||||r||||E_1||_G. \tag{65}$$

Hence, combining Eqn. (60), Eqn. (62), Eqn. (63), Eqn. (64) and Eqn. (65) into $\dot{V}^\sigma = \dot{V}_1^\sigma + \dot{V}_2^\sigma + \dot{V}_3^\sigma + \dot{V}_4^\sigma + \dot{V}_5^\sigma$ satisfies:

$$\begin{aligned}\dot{V}^\sigma \leq &-\left[\frac{1}{2}\underline{\alpha}(Q^{\sigma(t)}) - \frac{\bar{\alpha}(P^{\sigma(t)})\bar{\alpha}(A^{\sigma(t)})}{\underline{\alpha}(D^{\sigma(t)} + B^{\sigma(t)})}||\bar{\lambda}||\right]||r||^2\\ &+ \left[\frac{\bar{\alpha}(P^{\sigma(t)})\bar{\alpha}(A^{\sigma(t)})}{\underline{\alpha}(D^{\sigma(t)} + B^{\sigma(t)})}||\triangle||_G||\bar{\lambda}|| + \bar{\alpha}(P_1^{\sigma(t)})\right]||r||||E_1||_G\\ &+ \bar{\alpha}(P^{\sigma(t)})\bar{\alpha}(\nu_1 L + \nu_2 B)T_M||r|| - \kappa||\tilde{\theta}||_G^2 - \kappa_0||\tilde{\theta}_0||_{G_0^*}^2\\ &- \kappa_w||\tilde{\theta}_w||_{G_w}^2 + \Phi_n\bar{\alpha}(P^{\sigma(t)})\bar{\alpha}(A^{\sigma(t)})||\tilde{\theta}||_G||r||\\ &+ \Phi_{nw}\bar{\alpha}(P^{\sigma(t)})\bar{\alpha}(A^{\sigma(t)})||\tilde{\theta}_w||_{G_w}||r||\\ &+ \Phi_{n0}\bar{\alpha}(P^{\sigma(t)})\bar{\alpha}(A^{\sigma(t)})||\tilde{\theta}_0||_{G_0^*}||r||\\ &+ \bar{\alpha}(P^{\sigma(t)})\bar{\alpha}(\nu_1 L + \nu_2 B)T_N||r|| - \frac{\beta}{2}||E_1||_G^2 + \kappa\Theta_n||\tilde{\theta}||_G\\ &+ \kappa_w\Theta_{nw}||\tilde{\theta}_w||_{G_w} + \kappa_0\Theta_{n0}||\tilde{\theta}_0||_{G_0^*} + \frac{1}{2}cE_0\underline{\alpha}(Q^{\sigma(t)})||r||,\end{aligned} \tag{66}$$

with $T_M := \varepsilon + \epsilon_w - \epsilon_0$ and $T_N := \Gamma^0 M^0 + \Gamma^1 M_I^c + \Gamma^2 M_0^c$.

In the interest of keeping this paper concise, we have abbreviated the full Lyapunov-derivative summation calculation that leads to Eqn. (66). Eqn. (66) is simply the result of adding the derivative bounds for V_1–V_5 and then using Cauchy–Schwarz, eigenvalue, and Assumption 3.1 bounds to control every trace and cross-term. Concretely, the $-\frac{1}{2}r^\top P^{\sigma(t)} r$ term and its worst-case coupling bounds produce the leading $\|r\|^2$ coefficient; the remaining consensus and potentials combine with the $\dot{V}_5$ estimate to yield the $\|r\|\|E_1\|_G$

group; substituting the adaptation laws into $\dot{V}_2$–$\dot{V}_4$ generates the $-\kappa\|\tilde{\theta}\|^2$, $-\kappa_0\|\tilde{\theta}_0\|^2$, and $-\kappa_w\|\tilde{\theta}_w\|^2$ terms along with their $\Phi\|\tilde{\theta}\|\|r\|$ and $\kappa\Theta\|\tilde{\theta}\|$ residuals; and invoking $\|\phi_i\| \leq \Phi_n$, $\|\phi_0\| \leq \Phi_{n0}$, $\|\phi_{iw}\| \leq \Phi_{nw}$ ensures all remaining cross-terms can be absorbed into the defined $\Phi_n, \Theta_n, \Phi_{n0}, \Theta_{n0}, \Phi_{nw}, \Theta_{nw}$ constants.

We rewrite Eqn. (66) in the simplified form,

$$\dot{V}^{\sigma} = -V_z^{\sigma}(z) \leq -z^{\top}Kz + \omega^{\top}z \tag{67}$$

with

$$K = \begin{bmatrix} \frac{\beta}{2} & 0 & 0 & 0 & g \\ 0 & \kappa & 0 & 0 & \gamma_1 \\ 0 & 0 & \kappa_w & 0 & \gamma_2 \\ 0 & 0 & 0 & \kappa_0 & \gamma_3 \\ g & \gamma_1 & \gamma_2 & \gamma_3 & \mu_1 \end{bmatrix},$$

$$\omega = \Big[0, \kappa\Theta_n, \kappa_w\Theta_{nw}, \kappa_0\Theta_{n0}, \Lambda\Big]^{\top},$$

$$\Lambda = \bar{\alpha}(P^{\sigma(t)})\bar{\alpha}(\nu_1 L + \nu_2 B)(T_M + T_N) + \mu_2,$$

$$\mathfrak{h} = \frac{\bar{\alpha}(P^{\sigma(t)})\bar{\alpha}(A^{\sigma(t)})}{\underline{\alpha}(D^{\sigma(t)} + B^{\sigma(t)})}||\bar{\lambda}||,$$

$$\gamma_1 = -\frac{1}{2}\Phi_n\bar{\alpha}(P^{\sigma(t)})\bar{\alpha}(A^{\sigma(t)}),$$

$$\gamma_2 = -\frac{1}{2}\Phi_{nw}\bar{\alpha}(P^{\sigma(t)})\bar{\alpha}(A^{\sigma(t)}),$$

$$\gamma_3 = -\frac{1}{2}\Phi_{n0}\bar{\alpha}(P^{\sigma(t)})\bar{\alpha}(A^{\sigma(t)}),$$

$$\mu_1 = \frac{1}{2}\underline{\alpha}(Q^{\sigma(t)}) - \mathfrak{h},$$

$$\mu_2 = \frac{1}{2}cE_0\underline{\alpha}(Q^{\sigma(t)}),$$

$$\mathbf{g} = -\frac{1}{2}\left[\frac{\bar{\alpha}(P^{\sigma(t)})\bar{\alpha}(A^{\sigma(t)})}{\underline{\alpha}(D^{\sigma(t)} + B^{\sigma(t)})}||\triangle||_G||\bar{\lambda}|| + \bar{\alpha}(P_1^{\sigma(t)})\right],$$

$$z = \Big[||E_1||_G, ||\tilde{\theta}||_G, ||\tilde{\theta}_w||_{G_w}, ||\tilde{\theta}_0||_{G_0^*}, ||r||\Big]^{\top}. \tag{68}$$

$V_z^{\sigma}(z)$ is positive definite whenever the following two conditions are met; K is positive definite and $||z|| > \frac{||\omega||}{\underline{\alpha}(K)}$.

For the ***first condition*** to be satisfied, according to Sylvester's criterion, we must ensure $\beta > 0$, $\frac{\beta}{2}\kappa > 0$, $\frac{\beta}{2}\kappa\kappa_w > 0$, $\frac{\beta}{2}\kappa\kappa_w\kappa_0 > 0$, and $\frac{\beta}{2}\kappa\kappa_w(\kappa_0\mu_1 - \gamma_3^2) - \frac{\beta}{2}\kappa\gamma_2^2\kappa_0 - \frac{\beta}{2}\gamma_1^2\kappa_w\kappa_0 - \mathbf{g}^2\kappa\kappa_w\kappa_0 > 0$, with the isolation of μ_1, yields

$$\mu_1 > \frac{1}{\frac{\beta}{2}\kappa\kappa_w\kappa_0}\left[\frac{\beta}{2}\kappa\kappa_w\gamma_3^2 + \frac{\beta}{2}\kappa\gamma_2^2\kappa_0 + \frac{\beta}{2}\gamma_1^2\kappa_w\kappa_0 + \mathbf{g}^2\kappa\kappa_w\kappa_0\right]$$

For the ***second condition*** to be satisfied, we require $||z|| > B_d$, where

$$B_d = \frac{||\omega||_1}{\underline{\alpha}(K)} \tag{69}$$

with $\omega = \Big[0, \kappa\Theta_n, \kappa_w\Theta_{nw}, \kappa_0\Theta_{n0}, \Lambda\Big]^{\top}$ and $||\omega||_1 = \kappa\Theta_n + \kappa_w\Theta_{nw} + \kappa_0\Theta_{n0} + \Lambda$. Thus,

$$B_d = \frac{\kappa\Theta_n + \kappa_w\Theta_{nw} + \kappa_0\Theta_{n0} + \Lambda}{\underline{\alpha}(K)} \tag{70}$$

If $||z|| > B_d$, then $\dot{V}^{\sigma} \leq -V_z^{\sigma}(z)$ with $V_z^{\sigma}(z)$ being positive definite. Singular values are defined for all matrix dimensions. Using the singular value bounds:

$\underline{\sigma}(P^{\sigma(t)})\,\|r\|^2 \leq r^T P^{\sigma(t)} r \leq \bar{\sigma}(P^{\sigma(t)})\,\|r\|^2$,
$\frac{1}{\bar{\sigma}(G)}\,\|\tilde{\theta}\|_G^2 \leq \mathrm{tr}(\tilde{\theta}^T G^{-1}\tilde{\theta}) \leq \frac{1}{\underline{\sigma}(G)}\,\|\tilde{\theta}\|_G^2$,
$\frac{1}{\bar{\sigma}(G_0^*)}\,\|\tilde{\theta}_0\|_G^2 \leq \mathrm{tr}(\tilde{\theta}_0^T G_0^{*-1}\tilde{\theta}_0) \leq \frac{1}{\underline{\sigma}(G_0^*)}\,\|\tilde{\theta}_0\|_G^2$,
$\frac{1}{\bar{\sigma}(G_w)}\,\|\tilde{\theta}_w\|_G^2 \leq \mathrm{tr}(\tilde{\theta}_w^T G_w^{-1}\tilde{\theta}_w) \leq \frac{1}{\underline{\sigma}(G_w)}\,\|\tilde{\theta}_w\|_G^2$,
$\underline{\sigma}(P_1^{\sigma(t)})\,\|E_1\|_G^2 \leq \mathrm{tr}(E_1^T P_1^{\sigma(t)} E_1) \leq \bar{\sigma}(P_1^{\sigma(t)})\,\|E_1\|_G^2$.

Combining and halving gives $\frac{\underline{\sigma}(P^{\sigma(t)})}{2}\,\|r\|^2 + \frac{1}{2\,\bar{\sigma}(G)}\,\|\tilde{\theta}\|_G^2 + \frac{1}{2\,\bar{\sigma}(G_0^*)}\,\|\tilde{\theta}_0\|_G^2 + \frac{1}{2\,\bar{\sigma}(G_w)}\,\|\tilde{\theta}_w\|_G^2 + \frac{\underline{\sigma}(P_1^{\sigma(t)})}{2}\,\|E_1\|_G^2 \leq V^{\sigma} \leq \frac{\bar{\sigma}(P^{\sigma(t)})}{2}\,\|r\|^2 + \frac{1}{2\,\underline{\sigma}(G)}\,\|\tilde{\theta}\|_G^2 + \frac{1}{2\,\underline{\sigma}(G_0^*)}\,\|\tilde{\theta}_0\|_G^2 + \frac{1}{2\,\underline{\sigma}(G_w)}\,\|\tilde{\theta}_w\|_G^2 + \frac{\bar{\sigma}(P_1^{\sigma(t)})}{2}\,\|E_1\|_G^2$. Considering Eqn. (68), the inequality simplifies to

$$\underline{\alpha}(\eta)||z||^2 \leq V^{\sigma} \leq \bar{\alpha}(\zeta)||z||^2, \tag{71}$$

where

$$\eta = \mathrm{diag}\Big(\frac{\underline{\alpha}(P^{\sigma(t)})}{2}, \frac{1}{2\bar{\alpha}(G)}, \frac{1}{2\,\bar{\sigma}(G_0^*)}, \frac{1}{2\bar{\alpha}(G_w)}, \frac{\underline{\alpha}(P_1^{\sigma(t)})}{2}\Big)$$

and

$$\zeta = \mathrm{diag}\Big(\frac{\bar{\alpha}(P^{\sigma(t)})}{2}, \frac{1}{2\underline{\alpha}(G)}, \frac{1}{2\,\underline{\sigma}(G_0^*)}, \frac{1}{2\underline{\alpha}(G_w)}, \frac{\bar{\alpha}(P_1^{\sigma(t)})}{2}\Big).$$

Then for any initial $z(t_0)$, there exists T_0 such that

$$||z(t)|| \leq \sqrt{\frac{\bar{\alpha}(\zeta)}{\underline{\alpha}(\eta)}}B_d, \quad \forall t \geq t_0 + T_0. \tag{72}$$

Let $\mathcal{Z} = \min_{z||f||z|| \geq B_d} V_z^{\sigma}(z)$, then

$$T_0 = \frac{V^{\sigma}(t_0) - \bar{\alpha}(\zeta)(B_d)^2}{\mathcal{Z}}. \tag{73}$$

This implies $r(t)$ is ultimately bounded, which yields $e_i(t)$, $e^n(t)$, and δ^k CUUB, thus achieving synchronization over $\mathcal{G}$.

Part 2: We show that $x_i(t)$ is bounded $\forall t \geq t_0$ and $\forall i \in \mathbb{N}$. From Eqn. (67):

$$\dot{V}^{\sigma} \leq -\underline{\alpha}(K)||z||^2 + ||\omega||||z||. \tag{74}$$

which, together with *Eqn.* (71), we obtain

$$\frac{d}{dt}(\sqrt{V^{\sigma}}) \leq -\frac{\underline{\alpha}(K)}{2\bar{\alpha}(\zeta)}\sqrt{V^{\sigma}} + \frac{||\omega||}{2\sqrt{\underline{\alpha}(\eta)}}. \tag{75}$$

Thus, it follows from [27, Corollary 1.1], that $V^{\sigma}(t)$ remains bounded for all $t \geq t_0$. This results, together with Assumption 2.2, yields $\delta_i^k = (x_i^k - \psi_i^k) - (x_0^k - \psi_0^k)$ being CUUB, i.e., $||x_i|| \leq X_{\text{init}}$ and $||x_0|| \leq X_{0,\text{init}}$ are bounded $\forall t \geq t_0$. □

4.5 Proposed Average Dwell-Time Requirement. Section 4.4 established, for each fixed topology, a Lyapunov derivative bound that yields ultimate boundedness and CUUB of the tracking and adaptation errors. We now derive a sufficient average dwell-time condition ensuring that these mode-wise practical-stability estimates are preserved under topology switching.

A key distinction with the dwell time frameworks in [19,22], is that we derive explicit expressions (77) and (79) for the jump factor μ and the continuous-time dissipation rate ϱ_0 in a heterogeneous multi-agent setting that simultaneously handles online NN-based cancellation of unknown dynamics, collision and obstacle avoidance, and switching communication topologies. Critically, the derivation retains the residual term c_0 throughout, so the conclusion is uniform ultimate boundedness, consistent with the CUUB result of Theorem 4.1. Embedding these tailored expressions into our adaptive, safety-constrained, time-based switching framework extends previous dwell time works to this multi-agent context.

The following proposition combines the continuous-time interval estimate for the Lyapunov function with the topology-dependent jump bound at switching instants to obtain a sufficient lower bound on the average dwell time.

Proposition 4.2 (Average dwell-time condition for switched practical stability)**.** *Suppose that for each topology $\sigma \in \mathcal{M}$, the Lyapunov function V^σ satisfies*

$$\dot{V}^\sigma \le -\varrho_\sigma V^\sigma + c_\sigma, \tag{76}$$

with

$$\varrho_\sigma := \frac{\underline{\alpha}(K)}{2\bar{\alpha}(\zeta)} > 0, \qquad c_\sigma := \frac{\bar{\omega}^2}{2\underline{\alpha}(K)} \ge 0, \tag{77}$$

where $\bar{\omega}$ is a bound on the residual vector $\|\omega\|$ from Eqn. (67), K, ζ, and $\bar{\omega}$ are evaluated under the active topology σ. Assume further that at each switching instant t_s,

$$V^{\sigma(t_s^+)}(x(t_s^+)) \le \mu\, V^{\sigma(t_s^-)}(x(t_s^-)), \tag{78}$$

where the jump factor (taken over the pre-switch mode, σ^-, and the post-switch mode, σ^+)

$$\mu := \max_{\sigma^-,\sigma^+ \in \mathcal{M}} \frac{\bar{\alpha}(\zeta^{\sigma^+})}{\underline{\alpha}(\eta^{\sigma^-})} \ge 1, \tag{79}$$

where η and ζ are defined in Eqn. (71). Let $\varrho_0 := \min_{\sigma\in\mathcal{M}} \varrho_\sigma$. If the switching signal satisfies the average dwell-time bound

$$N^\sigma(\tau, t) \le N_0 + \frac{t-\tau}{\tau_a^*}, \qquad \forall t \ge \tau \ge t_0, \tag{80}$$

and

$$\tau_a^* > \frac{\ln \mu}{\varrho_0}, \tag{81}$$

then the switched closed-loop system is uniformly ultimately bounded.

Proof. Let $\{t_s\}_{s=0}^\infty$ be the strictly increasing sequence of switching instants, where $t_0 \ge 0$. At each t_s, the active topology switches to $\bar{\mathcal{G}}^{\sigma(t_s)}$. Assume for each admissible topology $\bar{\mathcal{G}}^{\mathcal{M}}$, there exists a continuously differentiable Lyapunov function $V^\sigma(x)$ (e.g., Eqn. (58)) that measures the consensus error of the agents under that topology. For brevity, at each switching instant t_s, we write $\sigma = \sigma(t_s)$, $\sigma^- = \sigma(t_s^-)$ topology just before the switch, , $\sigma^+ = \sigma(t_s^+)$ topology just after the switch, t_{s+1}^- means the value just before the time t_{s+1} and t_{s+1}^+ means just after the time t_{s+1} (similarly applies to t_s^- and t_s^+). Thus, $\mathcal{G}^\sigma$ will denote the active topology at t_s.

We start by evaluating the Lyapunov function across each switching instant. Specifically, we apply the special case of Young's inequality [28] to the fixed-mode Lyapunov estimate, Eqn. (74),

$$\dot{V}^\sigma \le -\underline{\alpha}(K)||z||^2 + ||\omega||||z|| \le -\frac{\underline{\alpha}(K)}{2}\|z\|^2 + \frac{||\omega||^2}{2\underline{\alpha}(K)}. \tag{82}$$

Together with Eqn. (71) upper-bound ($V^\sigma \le \bar{\alpha}(\zeta)\|z\|^2$), we obtain the scalar linear differential inequality

$$\dot{V}^\sigma \le -\varrho_\sigma V^\sigma + c_\sigma, \qquad \varrho_\sigma := \frac{\underline{\alpha}(K)}{2\bar{\alpha}(\zeta)}, \qquad c_\sigma := \frac{\bar{\omega}^2}{2\underline{\alpha}(K)}, \tag{83}$$

where $\bar{\omega}$ is a bound on the residual vector $\|\omega\|$ from Eqn. (67). Solving the ODE, Eqn. (83), with integrating factor $e^{\varrho_\sigma t}$ and integrating from t_s^+ to t_{s+1}^- on on each interval $[t_s, t_{s+1})$ is

$$V^\sigma(x(t_{s+1}^-)) \le e^{-\varrho_\sigma(t_{s+1}-t_s)} V^\sigma(x(t_s^+)) + \frac{c_\sigma}{\varrho_\sigma}\left(1 - e^{-\varrho_\sigma(t_{s+1}-t_s)}\right), \tag{84}$$

meaning we start from the state right after the previous switch, at t_s^+, then evolve continuously on $[t_s, t_{s+1})$, and bound the state right before the next switch at t_{s+1}^-.

The composite Lyapunov function is bounded as given by Eqn. (71) with topology-dependent constants $\underline{\alpha}(\eta)$ and $\bar{\alpha}(\zeta)$. When the topology switches from $\sigma(t_s^-)$ with bounds $(\underline{\alpha}(\eta^{(t_s^-)}), \bar{\alpha}(\zeta^{(t_s^-)}))$ to $\sigma(t_s^+)$ with bounds $(\underline{\alpha}(\eta^{(t_s^+)}), \bar{\alpha}(\zeta^{(t_s^+)}))$ at instant t_s, the state $x(t_s)$ is continuous (i.e., $x(t_s^+) = x(t_s^-)$), but the Lyapunov function changes because $P^{\sigma(t)}$, $Q^{\sigma(t)}$ and the adaptation-gain matrices change with the topology. Therefore the jump in the Lyapunov function is bounded by

$$V^\sigma(x(t_s^+)) \le \frac{\bar{\alpha}(\zeta^{(t_s^+)})}{\underline{\alpha}(\eta^{(t_s^-)})} V^{\sigma)}(x(t_s^-)).$$

Thus, the worst-case jump factor (taken over the pre-switch mode, σ^-, and the post-switch mode, σ^+) and worst-case constants over all topology pairs is

$$\mu := \max_{\sigma^-,\sigma^+ \in \mathcal{M}} \frac{\bar{\alpha}(\zeta^{\sigma^+})}{\underline{\alpha}(\eta^{\sigma^-})} \ge 1, \tag{85}$$

and we define

$$\varrho_0 = \min_{\sigma\in\mathcal{M}} \varrho_\sigma > 0 \qquad c_0 = \min_{\sigma\in\mathcal{M}} c_\sigma < \infty, \tag{86}$$

so that at every switching instant

$$V^\sigma(x(t_s^+)) \le \mu\, V^\sigma(x(t_s^-)). \tag{87}$$

Let $\{t_0, t_1, \dots, t_{N_\sigma(t_0,t)}\}$ be the switching instants on $[t_0, t]$ with $N^\sigma(t_0, t)$ the number of switches. The number of switches in $[t_0, t]$ is bounded by $N^\sigma(t_0, t)$ given by Eqn. (10). Applying Eqn. (84) over each interval and Eqn. (87) at each switch recursively, after the first interval and first switch (i.e., $s = 0$), we get

$$V^\sigma(x(t_1^+)) \le \mu\, e^{-\varrho_0(t_1-t_0)} V^\sigma(x(t_0)) + \mu\,\frac{c_0}{\varrho_0}\left(1 - e^{-\varrho_0(t_1-t_0)}\right). \tag{88}$$

Continuing recursively over $N^\sigma(t_0, t)$ switches yields

$$V^\sigma(x(t)) \le \mu^{N^\sigma} e^{-\varrho_0(t-t_0)} V^\sigma(x(t_0))$$

$$+\frac{c_0}{\varrho_0}\sum_{\jmath=0}^{N^\sigma-1}\mu^{N^\sigma-1-\jmath}e^{-\varrho_0(t-t_{\jmath+1})}(1-e^{-\varrho_0(t_1-t_0)}). \quad (89)$$

Rewriting the residual factor

$$\frac{1-e^{-\varrho_0\Delta_j}}{\varrho_0}=\int_{t_\jmath}^{t_{\jmath+1}}e^{-\varrho_0(t_{\jmath+1}-\tau)}\,d\tau, \quad (90)$$

and using in Eqn. (89) with $e^{-\varrho_0(t-t_{\jmath+1})}e^{-\varrho_0(t_{\jmath+1}-\tau)}=e^{-\varrho_0(t-\tau)}$,

$$V^\sigma(x(t))\le\mu^{N^\sigma}e^{-\varrho_0(t-t_0)}V^\sigma(x(t_0))$$
$$+c_0\sum_{\jmath=0}^{N^\sigma-1}\int_{t_\jmath}^{t_{\jmath+1}}\mu^{N^\sigma-\jmath}e^{-\varrho_0(t-\tau)}\,d\tau \quad (91)$$

But $\mu^{N^\sigma-\jmath}=\mu^{N^\sigma(\tau,t)}$ with $\tau\in[t_\jmath,t_{\jmath+1})$, hence,

$$V^\sigma(x(t))\le\mu^{N^\sigma}e^{-\varrho_0(t-t_0)}V^\sigma(x(t_0))$$
$$+c_0\int_{t_0}^{t_{N^\sigma}}\mu^{N^\sigma(\tau,t)}e^{-\varrho_0(t-\tau)}\,d\tau \quad (92)$$

For any $\tau\in[t_0,t]$, the number of switches in $[\tau,t]$ satisfies the average dwell-time condition

$$N^\sigma(\tau,t)\le N_0+\frac{t-\tau}{\tau_a^*}, \quad (93)$$

hence,

$$\mu^{N^\sigma(\tau,t)}e^{-\varrho_0(t-\tau)}\le\mu^{N_0}e^{-\left(\varrho_0-\frac{\ln\mu}{\tau_a^*}\right)(t-\tau)}. \quad (94)$$

Let

$$\hbar:=\varrho_0-\frac{\ln\mu}{\tau_a^*}. \quad (95)$$

Likewise, for the transient term, applying the average dwell time bound to $[t_0,t]$

$$\mu^{N^\sigma}e^{-\varrho_0(t-t_0)}\le\mu^{N_0}e^{-\hbar(t-t_0)} \quad (96)$$

hence,

$$V^\sigma(x(t))\le\mu^{N_0}e^{-\hbar(t-t_0)}V^\sigma(x(t_0))+\frac{c_0\mu^{N_0}}{\hbar}(1-e^{-\hbar(t-t_0)}). \quad (97)$$

Rather than handling each $V^\sigma(x(t))$ separately, we define the composite Lyapunov function

$$V(x(t))=\max_{\sigma\in\mathcal{M}}\left\{\iota^{\sigma(t)}V^\sigma(x(t))\right\}, \quad (98)$$

where $\iota^{\sigma(t)}\in(0,1]$ is a topology-dependent weighting scalar that depends on the algebraic connectivity of the graph $\bar{\mathcal{G}}^{\sigma(t)}$ defined as the second-smallest eigenvalue of its Laplacian matrix L^σ, denoted as $s_2(L^\sigma)$. The idea is to weight each topology's Lyapunov value by how well-connected that topology is. A topology with high algebraic connectivity (large $s_2(L^\sigma)$) gets a weight closer to 1, while a poorly connected topology gets a smaller weight. We choose

$$\iota^{\sigma(t)}=\frac{1}{1+\gamma\left(\kappa_{\max}-s_2(L^\sigma)\right)},$$

with $\gamma>0$ and $\kappa_{\max}=\max_{\sigma\in\mathcal{M}}s_2(L^\sigma)$ denoting the maximum algebraic connectivity across all admissible topology modes. Substituting Eqn. (97) into Eqn. (98) yields:

$$V(x(t))\ \le\ \left(\max_\sigma\iota^\sigma\right)\mu^{N_0}e^{-\hbar(t-t_0)}V(x(t_0))$$
$$+\left(\max_\sigma\iota^\sigma\right)\frac{c_0\mu^{N_0}}{\hbar}(1-e^{-\hbar(t-t_0)}). \quad (99)$$

If $\hbar>0$, Eqn. (99) requires

$$\tau_a^*>\frac{\ln\mu}{\varrho_0}. \quad (100)$$

Under condition Eqn.(100),

(1) The transient term $\left(\max_\sigma\iota^\sigma\right)\mu^{N_0}e^{-\hbar(t-t_0)}V(x(t_0))\to0$ as $t\to\infty$.
(2) The residual term converges to the finite limit $\left(\max_\sigma\iota^\sigma\right)\frac{c_0\mu^{N_0}}{\hbar}$ as $t\to\infty$.

Therefore, $V(x(t))$ is uniformly ultimately bounded with ultimate bound

$$\left(\max_\sigma\iota^\sigma\right)\frac{c_0\mu^{N_0}}{\hbar}. \quad (101)$$

Via the sandwich inequality, Eqn. (71), this translates to $\|z(t)\|$ converging to the residual set

$$\limsup_{t\to\infty}\|z(t)\|\ \le\ \sqrt{\frac{\left(\max_\sigma\iota^\sigma\right)c_0\,\mu^{N_0}}{\hbar\,\underline{\alpha}(\eta)}} \quad (102)$$

□

The proposed control and adaptation laws are fully distributed, allowing for online implementation without global knowledge of the graph or the states of non-neighboring agents. At runtime, an agent i requires only local information: its own state x_i, the states x_j of its current neighbors j where $(v_j,v_i)\in\mathcal{E}^{\sigma(t)}$, and the leader state x_0 whenever $b_{i0}^{\sigma(t)}\neq0$.

Several fixed design parameters are selected offline and stored as fixed design parameters. These include the Hurwitz design coefficients λ_k and the matrix $P_1^{\sigma(t)}$ satisfying Eqn. (36); the repulsion thresholds and saturation parameters appearing in Eqn. (7)–(9); the adaptation gain matrices Γ^0, Γ^1, and Γ^2; and the minimum average dwell time τ_a^* dictated by Eqn. (81). Additionally, strictly for stability analysis purposes, the graph-dependent matrices P^σ and Q^σ in Eqn. (38)–(39) are computed offline for each topological mode in $\mathcal{G}^{\mathcal{M}}$.

During online execution, each agent continuously computes the following at each time step: the synchronization errors e_i^k and weighted stability error r_i via Eqn. (27) and Eqn. (30); the NN weight estimates $\hat{\theta}_i$, $\hat{\theta}_{iw}$, and $\hat{\theta}_0$ via the tuning laws in Eqn. (53)–(54); the repulsive collision avoidance vectors $m_{ij}n_{ij}$, $m_{i0}n_{i0}$, and $m_{ic}n_{ic}$ via Eqn. (7)–(9), (42); and the overall control input u_i via Eqn. (41). Finally, because the leader determines and broadcasts the topology switching instants $\{t_s\}$ to the network, individual agents do not need to independently detect topological changes.

5 Numerical Example

We consider a network of agents composed of one leader and five heterogeneous followers, motivated by cooperative adaptive cruise control (CACC) [29]. The agents are required to maintain prescribed inter-agent spacings in the presence of bounded disturbances, and intermittent communication. To illustrate the proposed method, we use three control-oriented models: two-dimensional third-order systems in Example 1, two-dimensional second-order systems in Example 2 and one dimensional second-order systems in Example 3.

For all examples, communication between agents is via links that switch according to the four topologies in Figure 1 at random intervals, representing intermittent signal dropout.

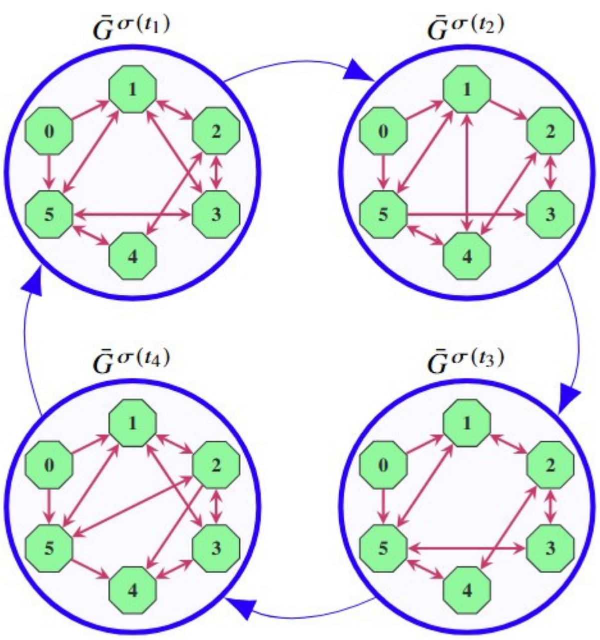

Fig. 1 The considered switching communication topology of the augmented graph $\bar{\mathcal{G}}$ in Section 5 illustrating different topologies at switching times t_1 to t_4. Leader is denoted by 0 and follower agents 1, 2, 3, 4 and 5

5.1 Example 1: Third-Order Agents in 2D Space. Each agent is modeled as a third-order point mass system with $n = 3$ and $p = 2$, where $x_i^1, x_i^2, x_i^3 \in \mathbb{R}^2$ denote position, velocity, and acceleration, respectively, and $\dot{x}_i^3$ is the jerk. Writing $x_i^1 = [x_i^{1,1}, x_i^{1,2}]^\top$, $x_i^2 = [x_i^{2,1}, x_i^{2,2}]^\top$, and $x_i^3 = [x_i^{3,1}, x_i^{3,2}]^\top$, the indices $\ell = 1, 2$ correspond to the longitudinal and lateral directions.

A stationary obstacle is placed at $O_c = [1.0, 1.5]^\top$, with detection radius $R = 1.5$ and exclusion radius $\mathfrak{L} = 0.5$. The desired formation offsets are $\psi_i^{1,1} = -1.1i$ and $\psi_i^{1,2} = 0$, corresponding to a longitudinal spacing of 1.1 units and zero lateral offset. For this example, we use 12-dimensional LIP bases for both the state $\phi_i(x_i)$ approximators: $\phi_i(x_i) = \big[1,\ x_i^{1,1},\ x_i^{1,2},\ x_i^{2,1},\ x_i^{2,2},\ x_i^{3,1},\ x_i^{3,2},\ (x_i^{1,1})^2,\ (x_i^{1,2})^2,$ $(x_i^{2,1})^2,\ (x_i^{2,2})^2,\ (x_i^{3,1})^2\big]^\top$ and disturbance $\phi_{iw}(t)$ approximators: $\phi_{iw}(t) = \big[1,\ \sin t,\ \cos t,\ \sin 2t,\ \cos 2t,\ \sin 3t,\ \cos 3t,$ $\sin^2 t,\ \cos^2 t,\ \sin t\,\cos t,\ e^{-t},\ t\,e^{-t}\big]^\top$. These bases provide a compact locally Lipschitz dictionary for approximating smooth nonlinearities and time-varying disturbances [24].

Leader: The dynamics of the leader is modeled as

$$\dot{x}_0^{1,1} = x_0^{2,1}, \quad \dot{x}_0^{1,2} = x_0^{2,2}; \quad \dot{x}_0^{2,1} = x_0^{3,1}, \quad \dot{x}_0^{2,2} = x_0^{3,2};$$

$$\dot{x}_0^{3,1} = -x_0^{2,1} - 2x_0^{3,1} + 1 + 3\sin(2\pi x_0^{1,1})$$
$$-\tfrac{1}{3}\big(x_0^{1,1} + x_0^{2,1} - 1\big)^2\big(x_0^{1,1} + 4x_0^{2,1} + 3x_0^{3,1} - 1\big),$$

$$\dot{x}_0^{3,2} = -x_0^{2,2} - 2x_0^{3,2} + 1 + 3\sin(2\pi x_0^{1,2})$$
$$-\tfrac{1}{3}\big(x_0^{1,2} + x_0^{2,2} - 1\big)^2\big(x_0^{1,2} + 4x_0^{2,2} + 3x_0^{3,2} - 1\big).$$

For each follower agent i ($i = 1, \ldots, 5$), the integrator chain is common:

$$\dot{x}_i^{1,\ell} = x_i^{2,\ell}, \qquad \dot{x}_i^{2,\ell} = x_i^{3,\ell}, \qquad \ell = 1, 2.$$

The follower jerk dynamics are $\dot{x}_i^{3,\ell} = f_i^\ell(x_i) + u_i^\ell + w_i^\ell(t)$, where f_i^ℓ models heterogeneous dynamics.

Agent 1:

$$\dot{x}_1^{3,1} = -0.08\,x_1^{2,1}x_1^{3,1} - 0.02\,(x_1^{2,1})^2 - 0.50\,x_1^{3,1} + u_1^1 + w_{x_1},$$

$$\dot{x}_1^{3,2} = -0.30\,x_1^{2,2} - 0.05\,(x_1^{2,2})^2 - 0.20\,x_1^{3,2} + u_1^2 + w_{y_1}.$$

Agent 2:

$$\dot{x}_2^{3,1} = -0.12\,x_2^{2,1}x_2^{3,1} - 0.035\,(x_2^{2,1})^2 - 0.60\,x_2^{3,1}$$
$$+ \frac{0.10\,(x_2^{2,1})^3}{1 + (x_2^{2,1})^2} + u_2^1 + w_{x_2},$$

$$\dot{x}_2^{3,2} = -0.40\,x_2^{2,2} - 0.08\,(x_2^{2,2})^2 - 0.25\,x_2^{3,2} + u_2^2 + w_{y_2}.$$

Agent 3:

$$\dot{x}_3^{3,1} = -0.10\,x_3^{2,1}x_3^{3,1} - 0.04\,(x_3^{2,1})^2 - 0.55\,x_3^{3,1}$$
$$+ 0.15\sin(x_3^{2,1}) + u_3^1 + w_{x_3},$$

$$\dot{x}_3^{3,2} = -0.35\,x_3^{2,2} - 0.06\,(x_3^{2,2})^2 - 0.22\,x_3^{3,2}$$
$$+ 0.05\sin(x_3^{2,2}) + u_3^2 + w_{y_3}.$$

Agent 4:

$$\dot{x}_4^{3,1} = -0.25\,x_4^{2,1}x_4^{3,1} - 0.08\,(x_4^{2,1})^2 - 0.80\,x_4^{3,1}$$
$$- 0.30\,(x_4^{2,1} - 1)^2\tanh(x_4^{2,1}) + u_4^1 + w_{x_4},$$

$$\dot{x}_4^{3,2} = -0.50\,x_4^{2,2} - 0.12\,(x_4^{2,2})^2 - 0.35\,x_4^{3,2} + u_4^2 + w_{y_4}.$$

Agent 5:

$$\dot{x}_5^{3,1} = -0.06\,x_5^{2,1}x_5^{3,1} - 0.015\,(x_5^{2,1})^2 - 0.40\,x_5^{3,1}$$
$$+ \frac{0.10\,x_5^{1,1}}{1 + (x_5^{1,1})^2} + u_5^1 + w_{x_5},$$

$$\dot{x}_5^{3,2} = -0.25\,x_5^{2,2} - 0.04\,(x_5^{2,2})^2 - 0.18\,x_5^{3,2} + u_5^2 + w_{y_5}.$$

5.2 Example 2: Second-Order Agents in 2D Space. Each agent is modeled as a second-order point-mass system in the longitudinal and lateral directions. The control objective remains spacing regulation with zero nominal lateral offset, except during obstacle-avoidance maneuvers.

Two stationary obstacles representing disabled agents are placed at $O_c = [200, 500; 1.5, 2.5]^\top$ along the path, with outer detection radius $R = 1.5$ and inner exclusion radius $\mathfrak{L} = 0.5$. The desired formation offsets are similar to that of Example 1 i.e., $\psi_i^{1,1} = -1.1i$ and $\psi_i^{1,2} = 0$. For this example, the state and disturbance approximators use the following LIP bases: $\phi_i(x_i) = \big[1,\ x_i^{1,1},\ x_i^{1,2},\ x_i^{2,1},\ x_i^{2,2},\ x_i^{3,1},\ x_i^{3,2},\ (x_i^{1,1})^2,\ (x_i^{1,2})^2\big]^\top$ and $\phi_{iw}(t) = \big[1,\ \sin t,\ \cos t,\ \sin 2t,\ \cos 2t,\ \sin 3t,\ \cos 3t,$ $\sin^2 t,\ \cos^2 t\big]^\top$.

Leader: The leader is modeled as

$$\dot{x}_0^{1,1} = x_0^{2,1}, \qquad \dot{x}_0^{1,2} = x_0^{2,2},$$

$$\dot{x}_0^{2,1} = -0.20\big(x_0^{2,1} - 26.8\big) - 0.10\tanh(x_0^{2,1}/0.5) - 0.0045\,x_0^{2,1} - 2.34\times10^{-4}\,x_0^{2,1}|x_0^{2,1}|,$$

$$\dot{x}_0^{2,2} = -0.30\,x_0^{1,2} - 0.85\,x_0^{2,2} - 0.008\,x_0^{2,1}x_0^{2,2}.$$

For each follower agent i ($i = 1, \ldots, 5$), we use the second-order model

$$\dot{x}_i^{1,1} = x_i^{2,1}, \qquad \dot{x}_i^{1,2} = x_i^{2,2},$$

$$\dot{x}_i^{2,1} = -c_{r,i}\tanh\left(\frac{x_i^{2,1}}{0.5}\right) - c_{v,i}x_i^{2,1} - k_{d,i}x_i^{2,1}|x_i^{2,1}| + u_i^1 + w_i^1(t),$$

$$\dot{x}_i^{2,2} = -k_{y,i}x_i^{1,2} - c_{y,i}x_i^{2,2} - k_{s,i}x_i^{2,1}x_i^{2,2} + u_i^2 + w_i^2(t),$$

where u_i^1 and u_i^2 are commanded longitudinal and lateral accelerations.

Agent 1:

$$\dot{x}_1^{2,1} = -0.103\tanh(x_1^{2,1}/0.5) - 0.0045\,x_1^{2,1} - 2.45\times10^{-4}\,x_1^{2,1}|x_1^{2,1}| + u_1^1 + w_{x_1},$$

$$\dot{x}_1^{2,2} = -0.35\,x_1^{1,2} - 0.80\,x_1^{2,2} - 0.008\,x_1^{2,1}x_1^{2,2} + u_1^2 + w_{y_1}.$$

Agent 2:

$$\dot{x}_2^{2,1} = -0.108\tanh(x_2^{2,1}/0.5) - 0.0050\,x_2^{2,1} - 2.51\times10^{-4}\,x_2^{2,1}|x_2^{2,1}| + u_2^1 + w_{x_2},$$

$$\dot{x}_2^{2,2} = -0.32\,x_2^{1,2} - 0.90\,x_2^{2,2} - 0.009\,x_2^{2,1}x_2^{2,2} + u_2^2 + w_{y_2}.$$

Agent 3:

$$\dot{x}_3^{2,1} = -0.113\tanh(x_3^{2,1}/0.5) - 0.0055\,x_3^{2,1} - 2.45\times10^{-4}\,x_3^{2,1}|x_3^{2,1}| + u_3^1 + w_{x_3},$$

$$\dot{x}_3^{2,2} = -0.28\,x_3^{1,2} - 0.95\,x_3^{2,2} - 0.010\,x_3^{2,1}x_3^{2,2} + u_3^2 + w_{y_3}.$$

Agent 4:

$$\dot{x}_4^{2,1} = -0.070\tanh(x_4^{2,1}/0.5) - 0.0025\,x_4^{2,1} - 2.45\times10^{-4}\,x_4^{2,1}|x_4^{2,1}| + u_4^1 + w_{x_4},$$

$$\dot{x}_4^{2,2} = -0.22\,x_4^{1,2} - 1.05\,x_4^{2,2} - 0.012\,x_4^{2,1}x_4^{2,2} + u_4^2 + w_{y_4}.$$

Agent 5:

$$\dot{x}_5^{2,1} = -0.088\tanh(x_5^{2,1}/0.5) - 0.0040\,x_5^{2,1} - 1.87\times10^{-4}\,x_5^{2,1}|x_5^{2,1}| + u_5^1 + w_{x_5},$$

$$\dot{x}_5^{2,2} = -0.40\,x_5^{1,2} - 0.75\,x_5^{2,2} - 0.007\,x_5^{2,1}x_5^{2,2} + u_5^2 + w_{y_5}.$$

5.3 Example 3: Vehicle Platoon in a Single Lane. We consider a one-dimensional longitudinal platoon consisting of one lead agent and five heterogeneous follower agents. In this example, each agent is modeled as a second-order point-mass system with $n = 2$ and $p = 1$, where $x_i^1 \in \mathbb{R}$ denotes the longitudinal position and $x_i^2 \in \mathbb{R}$ denotes the longitudinal velocity. This example therefore focuses on longitudinal spacing regulation under switching communication topologies and bounded external disturbances.

For this 1D example, we use a 5-dimensional LIP basis for the state approximators: $\phi_i(x_i) = \big[1,\ x_i^1,\ x_i^2,\ (x_i^1)^2,\ (x_i^2)^2\big]^\top$, and a 5-dimensional disturbance basis: $\phi_{iw}(t) = \big[1,\ \sin t,\ \cos t,\ \sin 2t,\ \cos 2t\big]^\top$. The desired formation offsets is $\psi_i^1 = -1.1i$.

Leader: The leader agent is modeled as:

$$\dot{x}_0^1 = x_0^2,$$

$$\dot{x}_0^2 = -0.20\big(x_0^2 - 26.8\big) - 0.10\big(x_0^2/0.5\big) - 0.0045\,x_0^2 - 2.34\times10^{-4}\,x_0^2|x_0^2|.$$

For each follower agent i ($i = 1, \ldots, 5$), the common integrator structure is

$$\dot{x}_i^1 = x_i^2,$$

and the longitudinal acceleration dynamics are modeled as

$$\dot{x}_i^2 = f_i(x_i) + u_i + w_i(t),$$

where $u_i \in \mathbb{R}$ is the control input and $w_i(t) \in \mathbb{R}$ is a bounded time-varying disturbance.

We consider the following car model for all vehicles:

$$\begin{cases} \dot{x}_i^1 = x_i^2 \\ \dot{x}_i^2 = \dfrac{1}{m_i}\left(-gC_{r,i}x_i^2 - \dfrac{\rho C_{d,i}A_{f,i}}{2}x_i^2|x_i^2| + G_i(u_i + w_i)\right), \end{cases}$$

with $\rho = 1.225\,\text{kg/m}^3$, $g = 9.81 m/s^2$, $C_{r,1} = 0.01096, C_{r,2} = 0.01152, C_{r,3} = 0.01208, C_{r,4} = 0.00739, C_{r,5} = 0.00938$

Agent 1 (Compact car: $m_1 \approx 1500\,\text{kg}$, $C_{d,1}A_{f,1} \approx 0.60\,\text{m}^2$):

$$\dot{x}_1^2 = -0.103x_1^2 - 0.0045\,x_1^2 - 2.45\times10^{-4}\,x_1^2|x_1^2| + G_1(u_1 + w_1(t)).$$

Agent 2 (SUV: $m_2 \approx 2200\,\text{kg}$, $C_{d,2}A_{f,2} \approx 0.90\,\text{m}^2$):

$$\dot{x}_2^2 = -0.108x_2^2 - 0.0050\,x_2^2 - 2.51\times10^{-4}\,x_2^2|x_2^2| + G_2(u_2 + w_2(t)).$$

Agent 3 (Light truck: $m_3 \approx 2500\,\text{kg}$, $C_{d,3}A_{f,3} \approx 1.00\,\text{m}^2$):

$$\dot{x}_3^2 = -0.113x_3^2 - 0.0055\,x_3^2 - 2.45\times10^{-4}\,x_3^2|x_3^2| + G_3(u_3 + w_3(t))$$

Agent 4 (Heavy truck: $m_4 \approx 15000\,\text{kg}$, $C_{d,4}A_{f,4} \approx 6.00\,\text{m}^2$**):**

$$\dot{x}_4^2 = -0.070x_4^2 - 0.0025\,x_4^2 - 2.45 \times 10^{-4}\,x_4^2|x_4^2| + G_4(u_4 + w_4(t)).$$

Agent 5 (Electric vehicle: $m_5 \approx 1800\,\text{kg}$, $C_{d,5}A_{f,5} \approx 0.55\,\text{m}^2$**):**

$$\dot{x}_5^2 = -0.088x_5^2 - 0.0040\,x_5^2 - 1.87 \times 10^{-4}\,x_5^2|x_5^2| + G_5(u_5 + w_5(t)).$$

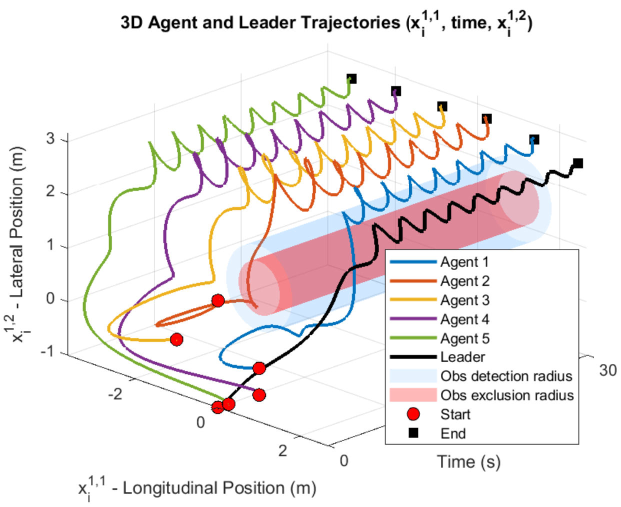

(a) Example 1 - 3D Leader and Follower Agents state components

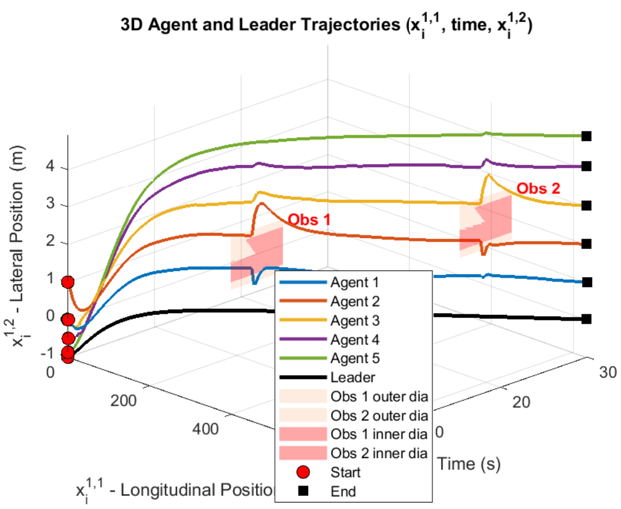

(b) Example 2 - 3D Leader and Follower Agents state components

Fig. 2 The corresponding evolution of the positional states $x_i^1 \in \mathbb{R}^2$, for the leader $i = 0$, follower agents $i \in \{1, 2, \cdots, 5\}$.

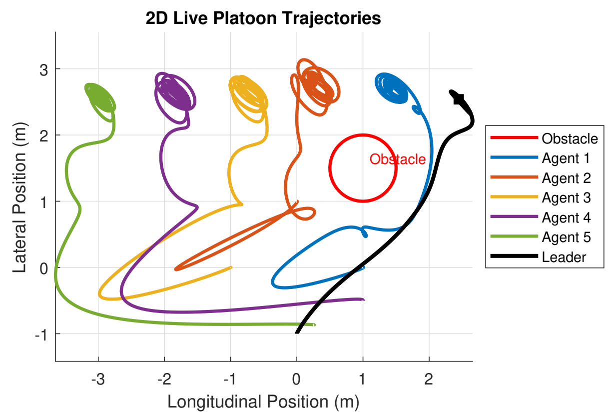

(a) Example 1 - 2D Leader and Follower Agents state components

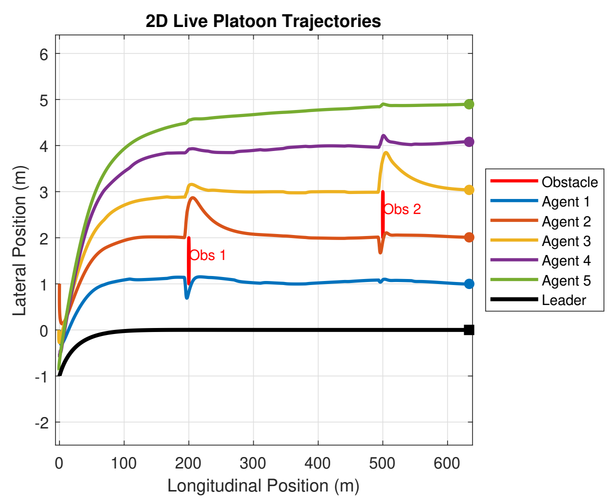

(b) Example 2 - 2D Leader and Follower Agents state components

Fig. 3 Time evolution of the position state (agents vs. leader).

5.4 Results. Figures 2–3 show that the proposed strategy maintains coordinated and collision-free behavior under heterogeneous dynamics and switching communication. In Example 1, Figures 5(a) and 6(a), the third-order model exhibits stronger transient oscillations, especially during the initial maneuver and topology switches, but the follower trajectories remain bounded and converge to the desired formation with small residual oscillations. The corresponding relative position errors in both longitudinal and lateral directions settle to bounded neighborhoods of their desired values, indicating satisfactory tracking despite heterogeneous jerk dynamics and disturbances.

In Example 2, Figures 5(b) and 6(b), the second-order model produces smoother longitudinal evolution but larger lateral excursions, with visible slope changes in the lateral states when the

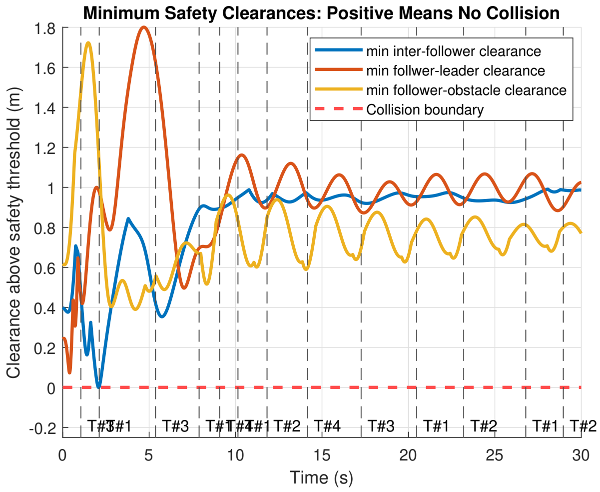

(*a*) Example 1 - Minimum Safety Clearances

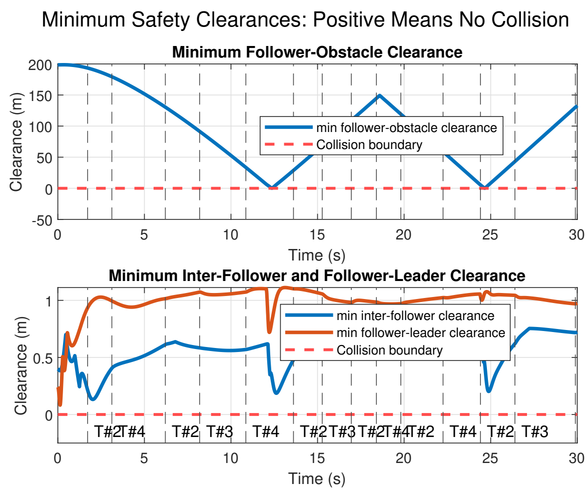

(*b*) Example 2 - Minimum Safety Clearances

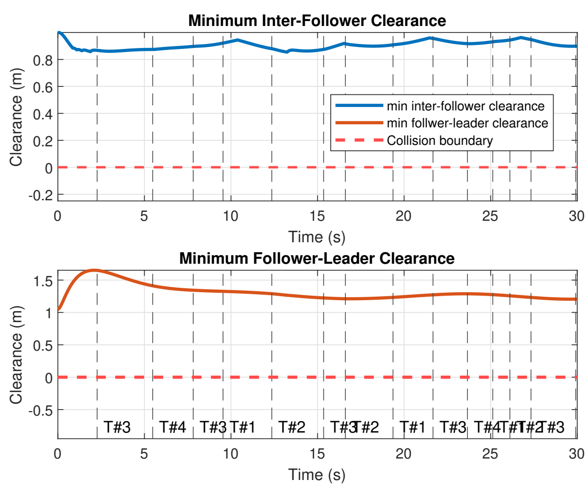

(*c*) Example 3 - Minimum Safety Clearances

Fig. 4 The leader $i = 0$, follower agents $i \in \{1, 2, \cdots, 5\}$ and obstacles minimum safety clearances.

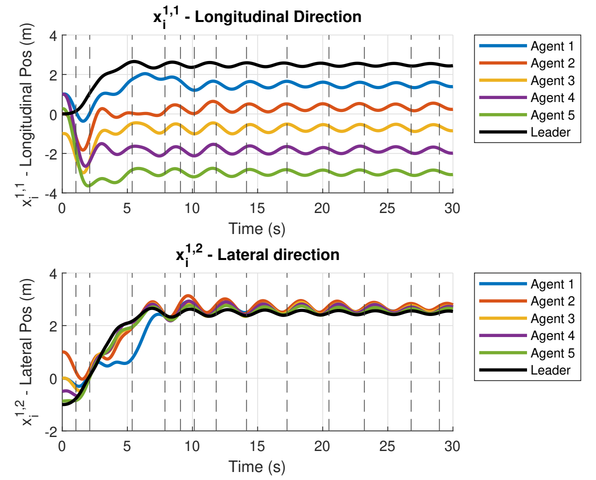

(*a*) Example 1 - relative x_i^1 state Error between Agents and Leader

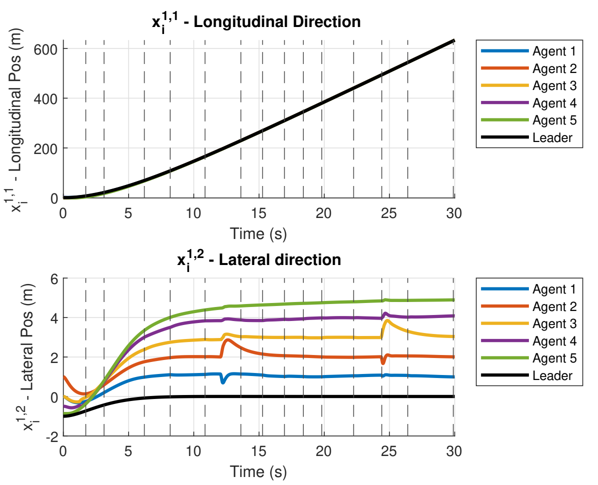

(*b*) Example 2 - relative x_i^1 state Error between Agents and Leader

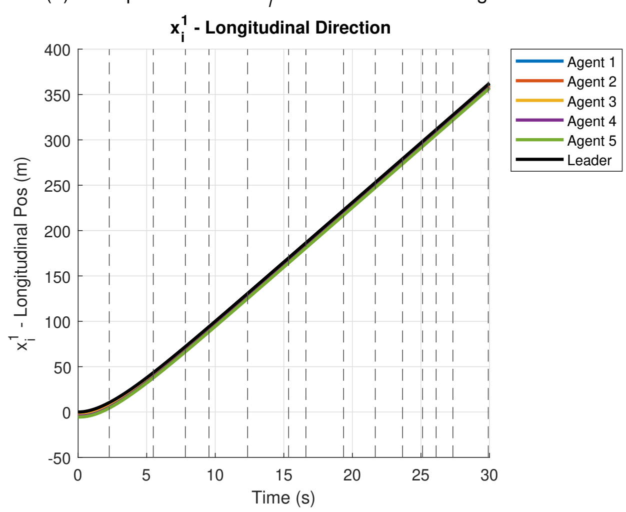

(*c*) Example 3 - relative x_i^1 state Error between Agents and Leader

Fig. 5 Time evolution of the leader and follower position state.

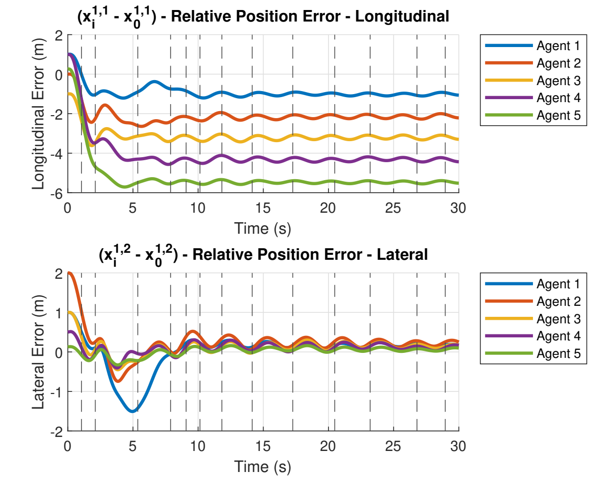

(*a*) Example 1 - relative state Error between Agents and Leader

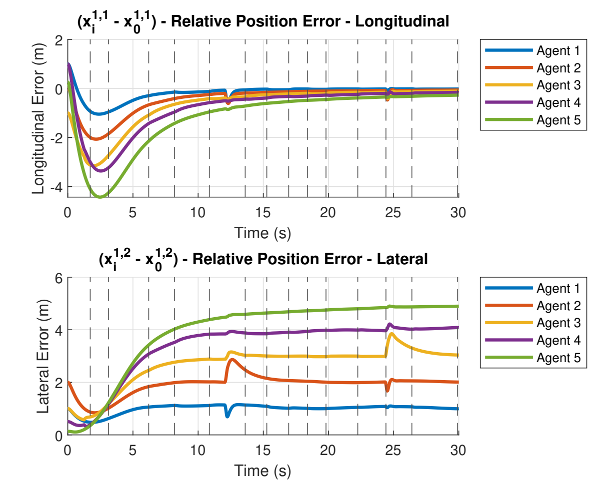

(*b*) Example 2 - relative state Error between Agents and Leader

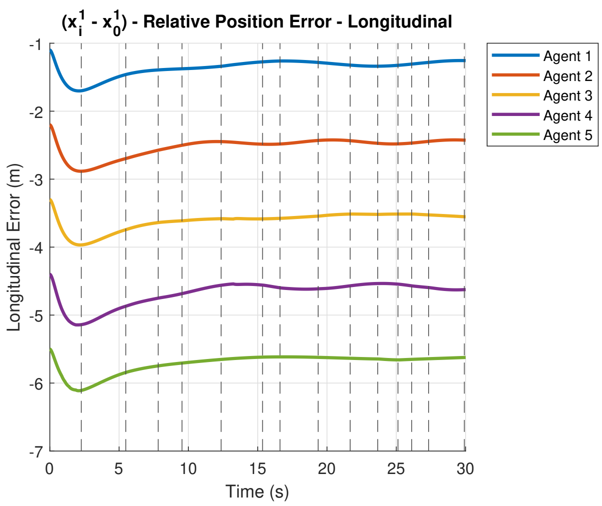

(*c*) Example 3 - relative state Error between Agents and Leader

Fig. 6 Time evolution of the relative position state error (agents vs. leader).

obstacle-avoidance action becomes active. In both cases, the minimum inter-follower, follower-leader, and follower-obstacle clearances remain positive, confirming safe operation throughout the maneuver.

Whereas Examples 1 and 2 emphasize coupled longitudinal-lateral coordination with obstacle avoidance, Example 3 is included to isolate the longitudinal string-formation behavior of the proposed controller. Example 3 isolates the one-dimensional longitudinal vehicle platooning problem and therefore highlights the spacing-regulation performance without lateral avoidance effects. As seen in Figure 5(*c*), all follower longitudinal positions evolve smoothly with the leader trajectory, while Figure 6(*c*) shows that the relative longitudinal errors undergo an initial transient dip and then recover to constant ordered offsets consistent with the desired platoon formation. The corresponding safety plots in Figure 4(*c*) further show that both the minimum inter-follower clearance and the minimum follower-leader clearance remain strictly positive for all time, confirming collision-free longitudinal coordination. Compared with Examples 1 and 2, Example 3 exhibits the cleanest transient behavior, since no lateral re-routing or obstacle-induced switching is present.

The kinks visible in Figures 2 and 5 are caused by the activation of obstacle-avoidance maneuvers, and they appear most clearly in the lateral position because the avoidance action is realized primarily through lateral deviation. In Figure 5(*a*), the most noticeable lateral kink occurs around $t \approx 5$ s for Agent 1, which is the follower whose trajectory passes closest to the obstacle in Figure 3(*a*). In Figure 5(*b*), more pronounced lateral kinks appear around $t \approx 13$ s and $t \approx 24$ s, mainly for Agents 1–3, as their trajectories approach Obstacles 1 and 2 in Figure 3(*b*). Agent 4 shows only a smaller lateral perturbation, which is likely induced indirectly through inter-agent collision-avoidance and platoon-coupling effects rather than a direct obstacle encounter. Hence, these kinks should be interpreted as expected signatures of obstacle-triggered switching in the closed-loop motion, not as numerical artifacts or loss of stability.

The safety plots in Figure 4 further confirm collision-free performance in both cases. For Example 1 in Figure 4(*a*), the minimum inter-follower, follower-leader, and follower-obstacle clearances remain strictly positive, although some margins approach zero during the most demanding transient intervals. For Example 2 in Figure 4(*b*), the obstacle clearance stays comfortably positive, while the inter-follower and follower-leader clearances experience transient dips but never violate the collision boundary. Overall, the results show that the proposed strategy preserves formation structure and safety despite agent heterogeneity, switching topologies, and obstacle-induced maneuvers.

6 Conclusion

This paper has presented a distributed adaptive control strategy for uncertain leader-follower multi-agent systems operating under time-triggered switchings of communication topologies. By addressing the challenges posed by heterogeneous nonlinear dynamics, unknown parameters in dynamics, external disturbances, and evolving communication structures, the proposed framework ensures adaptive synchronization, formation maintenance, and stability in dynamic environments. The integration of neural network-based estimation techniques with adaptive tuning laws allows agents to effectively handle uncertainties in their dynamics and disturbances, while potential functions provide repulsion-based collision and obstacle mitigation within the control design.

Using a composite Lyapunov analysis framework that accounts for switching communication topologies, we formally established the stability and convergence properties of the proposed control laws under time-triggered communication transitions. The average dwell-time condition served as a critical constraint for ensuring smooth inter-topology transitions while preserving CUUB. Numerical simulations further demonstrated the efficacy of the approach, highlighting its ability to achieve coordinated motion and to suppress relative position errors even under reduced connectivity scenarios.

To broaden the applicability and enhance the practicality of our framework, several avenues for future work are apparent. First, while our analysis focuses on systems whose dynamics decompose into integrator chains plus locally Lipschitz nonlinearities, extending the method to encompass rigid-body models, input delays, or more intricate coupling structures would be valuable. Second, stability relies on an average-dwell-time constraint on topology switching; scenarios involving prolonged or arbitrary disconnects fall outside our guarantees. Third, incorporating control barrier functions for collision and obstacle avoidance will guard against potential chattering or oscillations induced by repulsive potentials, ensuring that control inputs remain within hardware limits. Finally, exploring reduced-order or sparsely parameterized basis function sets for the neural approximators may strike an even better balance between approximation accuracy and computational load, facilitating deployment on resource-constrained platforms. Further research directions include extensions to event-triggered switching of communication topologies, incorporating learning-based methods for topology optimization, and real-world implementations in applications such as autonomous vehicles, UAV swarms, and robotic teams. Collectively, these enhancements promise to extend our theoretical guarantees into a wider range of real-world multi-agent applications while addressing the computational and practical constraints inherent in distributed systems.

References

[1] Lewis, F. L., Zhang, H., Hengster-Movric, K., and Das, A., 2013, *Cooperative Control of Multi-Agent Systems: Optimal and Adaptive Design Approaches*, Springer.

[2] Ren, W. and Beard, R., 2005, "Consensus seeking in multiagent systems under dynamically changing interaction topologies," IEEE Transactions on Automatic Control, **50**(5), pp. 655–661.

[3] Khoo, S., Xie, L., and Man, Z., 2009, "Robust Finite-Time Consensus Tracking Algorithm for Multirobot Systems," IEEE Transactions on Mechatronics, **14**, pp. 219–228.

[4] Hong, Y., Hu, J., and Gao, L., 2006, "Tracking Control for Multi-Agent Consensus with an Active Leader and Variable Topologies," Automatica, **42**(7), pp. 1177–1182.

[5] Qin, J., Gao, H., and Wei, W., 2011, "Consensus Control for Multi-Agent Systems with Switching Topologies and Time-Varying Delays," IEEE Transactions on Automatic Control, **56**(5), pp. 1245–1250.

[6] Olfati-Saber, R., 2006, "Flocking for Multi-Agent Dynamic Systems: Algorithms and Theory," IEEE Transactions on Automatic Control, **51**(3), pp. 401–420.

[7] Wang, J. and Xin, M., 2011, "Multi-agent consensus algorithm with obstacle avoidance via optimal control approach," *Proceedings of the 2011 American Control Conference*, pp. 2783–2788, doi: 10.1109/ACC.2011.5990850.

[8] Lin, Z., Francis, B., and Maggiore, M., 2005, "Necessary and Sufficient Graphical Conditions for Formation Control of Unicycles," IEEE Transactions on Automatic Control, **50**(1), pp. 121–127.

[9] Moreau, L., 2005, "Stability of Multi-Agent Systems with Time-Dependent Communication Links," IEEE Transactions on Automatic Control, **50**(2), pp. 169–182.

[10] Shi, G. and Hong, Y., 2009, "Global Target Aggregation and State Agreement of Nonlinear Multi-Agent Systems with Switching Topologies," Automatica, **45**(5), pp. 1205–1211.

[11] Guo, S. and Xie, L., 2024, "Adaptive Neural Consensus of Unknown Non-Linear Multi-Agent Systems with Communication Noises under Markov Switching Topologies," Mathematics, **12**(1).

[12] Cao, X. and Li, Y., 2021, "Positive consensus for multi-agent systems with average dwell time switching," Journal of the Franklin Institute, **358**(16), pp. 8308–8329.

[13] Wu, X., Mao, B., Wu, X., and Lu, J., 2022, "Dynamic Event-Triggered Leader-Follower Consensus Control for MultiAgent Systems," SIAM Journal on Control and Optimization, **60**(1), pp. 189–209.

[14] Luo, X., Wang, J., Feng, J., Cai, J., and Zhao, Y., 2023, "Dynamic Event-Triggered Consensus Control for Markovian Switched Multi-Agent Systems: A Hybrid Neuroadaptive Method," Mathematics, **11**(9).

[15] Zhao, Z., Zhu, M., and Qin, J., 2023, "Adaptive Robust Time-Varying Formation Control of Quadrotors under Switching Topologies: Theory and Experiment," Aerospace, **10**(8).

[16] Li, J., Yan, Z., Shi, X., and Luo, X., 2024, "Distributed Adaptive Formation Control for Fractional-Order Multi-Agent Systems with Actuator Failures and Switching Topologies," Fractal and Fractional, **8**(10).

[17] Koulong, A. and Pakniyat, A., 2025, "Distributed Adaptive Consensus with Obstacle and Collision Avoidance for Networks of Heterogeneous Multi-Agent Systems," *2025 American Control Conference (ACC)*, pp. 3602–3607, doi: 10.23919/ACC63710.2025.11107682.

[18] Hespanha, J. P., Naghshtabrizi, P., and Xu, Y., 2007, "Networked control systems: Analysis and design," Proceedings of the IEEE, **95**(1), pp. 138–162.

[19] Liberzon, D., 2003, *Switching in Systems and Control*, Birkhäuser, Boston, MA.

[20] Ren, W., 2006, "Consensus based formation control strategies for multi-vehicle systems," *2006 American Control Conference*, pp. 6 pp.–, doi: 10.1109/ACC.2006.1657384.

[21] Tanner, H. G., Jadbabaie, A., and Pappas, G. J., 2007, "Flocking in Fixed and Switching Networks," IEEE Transactions on Automatic Control, **52**(5), pp. 863–868.

[22] Hespanha, J. and Morse, A., 1999, "Stability of switched systems with average dwell-time," *Proceedings of the 38th IEEE Conference on Decision and Control*, Vol. 3, pp. 2655–2660 vol.3, doi: 10.1109/CDC.1999.831330.

[23] Yesildirak, A., Lewis, F. W., and Jagannathan, S., 1995, *Neural Network Control of Robot Manipulators and Non-Linear Systems*, Taylor & Francis, London, UK.

[24] Brunton, S. L., Proctor, J. L., and Kutz, J. N., 2016, "Discovering governing equations from data by sparse identification of nonlinear dynamical systems," Proceedings of the National Academy of Sciences, **113**(15), pp. 3932–3937.

[25] Qu, Z., 2009, *Cooperative Control of Dynamical Systems: Applications to Autonomous Vehicles*, Springer-Verlag, London.

[26] Shivakumar, P. N. and Chew, K. H., 1974, "A sufficient condition for nonvanishing of determinants," Proceedings of the American Mathematical Society, **43**(1), pp. 63–66.

[27] Ge, S. and Wang, C., 2004, "Adaptive neural control of uncertain MIMO nonlinear systems," IEEE Transactions on Neural Networks, **15**(3), pp. 674–692.

[28] Young, W. H., 1912, "On classes of summable functions and their Fourier Series," Proceedings of the Royal Society of London. Series A, Containing Papers of a Mathematical and Physical Character, **87**(594), pp. 225–229.

[29] Coppola, A., Lui, D. G., Petrillo, A., and Santini, S., 2023, "Cooperative driving of heterogeneous uncertain nonlinear connected and autonomous vehicles via distributed switching robust PID-like control," Information Sciences, **625**, pp. 277–298.

List of Figures

List of Tables